Sādhanā (2020)45:142
https://doi.org/10.1007/s12046-020-01385-3

Multi-objective optimization in geometric design of tapered roller bearings based on fatigue, wear and thermal considerations through genetic algorithms

MEDURI KALYAN, RAJIV TIWARI* and MD SAIF AHMAD

Department of Mechanical Engineering, Indian Institute of Technology Guwahati, Guwahati, Assam 781039, India
e-mail: rtiwari@iitg.ac.in

MS received 27 October 2018; revised 17 March 2020; accepted 20 March 2020

Abstract. To improve the fatigue, wear and thermal based failures of Tapered Roller Bearings (TRBs) a multi-objective optimization technique has been proposed. Objective functions considered are: the dynamic capacity (C_d) that is related to fatigue life, the elasto-hydrodynamic minimum film thickness (h_{min}) that is associated to the wear life, and the maximum bearing temperature (T_{max}) that is related to the lubricant life. This paper presents a non-linear constrained optimization problem of three objectives with eleven design variables and twenty-eight constraints. The said objectives have been optimized individually (i.e., the single-objective optimization) and concurrently (i.e., the multi-objective optimization) through a multi-objective evolutionary procedure, titled as the Elitist Non-dominated Sorting Genetic Algorithm. A set of standard TRBs have been selected for the optimization. Pareto-optimal fronts (POFs) and Pareto-optimal surfaces (POSs) are obtained for one representative standard TRB. Out of many solutions on the POFs/POSs only the knee-point solution has been shown in a tabular form. Life comparison factors have been calculated based on both the optimized and standard TRBs, and results indicate that the optimized TRBs got enhanced lives than standard bearings. To get the graphical impression of optimized TRBs, a skeleton of radial dimensions of all seven optimized bearings based on various combinations of objectives has been shown for one of the representative standard TRB. In few cases the multi-objective optimization has better convergence as compared to single objective optimization due to its inherent diversity by the principle of dominance. The sensitivity investigation has also been conducted to observe the sensitivity of three objectives with design variables. From the sensitivity analysis data, tolerances have been provided for design variables. These tolerances could be used by the manufacturing industry while producing TRBs.

Keywords. Tapered roller bearings; dynamic capacity; elasto-hydrodynamic lubrication; maximum temperature; multiple objectives; NSGA-II; sensitivity analysis.

1. Introduction

Antifriction (rolling) bearings are commonly utilized to provide the spin, swaying and rectilinear motions of an object comparative to another. Antifriction bearings may be mostly categorized as the ball and roller bearings. Different shapes of rollers, like the cylindrical, tapered, spherical, and needle emanates underneath the roller bearing class. TRBs are known to carry either combined radial and thrust loads or pure thrust loads at medium speeds. TRBs with larger contact angles are used to carry heavy axial loads. Due to the presence of large sliding friction between roller ends and the cone back-face rib, TRBs are not suitable for high-speed applications. But recently, high-speed TRBs have been successfully developed through improvements of the guide lubrication. Double or four- row TRBs are used in heavy-axial load applications. Apart from axial loads, it encounters the preload, radial load and couple. It leads to the misalignment or slackness, when the preload value is reduced. TRBs are extensively used in rolling mills, agricultural machinery, machine tool spindles, axle boxes of rail vehicles, front and rear wheels of trucks and among others. To provide excellent performance, TRBs must have long fatigue life and wear life.

Andreason [1] described a method to calculate bearing loads in a two-row TRB arrangement by taking into account of the misalignment, initial preload, and deflections of the shaft and the housing. To determine the nature of the coefficient of friction at the large-rib roller end of a TRB, Karna [2] presented the analytical and experimental works.

*For correspondence
Published online: 03 June 2020

Liu [3] presented an analytical study to determine the load distribution in TRBs that operates under high speeds, combined loadings and negligible frictional forces. Bercea *et al* [4] gave an analytical model to predict the performances of double-row TRBs. A quasi-static analysis was used to determine the bearing stiffness, the fatigue life and the internal load distribution. Blake and Truman [5] proposed an experimental arrangement to measure the running torque of TRB under combined axial and radial loads. Results obtained are compared with the standard torque prediction model for TRBs.

Here the key research works associated to the optimization of antifriction bearing design will be deliberated. Chakraborty *et al* [6] optimized the dynamic load rating of ball bearings with five design variables and eight dissimilarity constraints through genetic processes. The constraint multi-objective optimization of ball bearings was accomplished by Gupta *et al* [7]. Considering the static load rating, dynamic load rating and minimum film-thickness as objectives, the multi-objective optimization was implemented through NSGA-II (Non-dominated Sorting Genetic Algorithm). A sensitivity investigation was furthermore executed on bearing objective functions. It was perceived that the static and dynamic load ratings are related. Rao and Tiwari [8] established a design procedure to optimize the deep-groove ball bearing taking the maximization of fatigue life as the objective. Kumar *et al* [9] implemented the single-objective constrained optimization on cylindrical roller bearings by considering the maximization of dynamic load rating as the objective. The constraint violation analysis was as well accomplished. Kumar *et al* [10] expressed the non-linear constrained optimization formulation for the crowned cylindrical roller bearing with logarithmic contours. The optimization was executed through utilizing real-coded genetic processes by considering the maximization of fatigue life as the objective expression.

Lin [11] optimized deep-groove ball bearings by utilizing binary-coded genetic algorithms (BGA) and the Genetic Algorithm-Differential Evolution hybrid algorithm (GA-DE). From the analysis, it was found that the GA-DE could give better results than the BGA. Wang *et al* [12] developed a mathematical model to optimized TRB. The proposed design gave an increase in dynamic capacity by 22% and the working life expectancy by 85% when compared to standard four column TRBs. Tiwari *et al* [13] optimized the dynamic capacity of TRBs through real coded genetic algorithms. Simply one objective, i.e., the dynamic capacity, and twenty-six constraints were considered for the optimization. In fact, to convey actual operating conditions and geometrical constraints of TRBs, even more objectives and constraints are needed.

Waghole and Tiwari [14] accomplished the optimization of needle roller bearings (NRBs) by taking single objective (i.e., the maximization of dynamic load rating) and sixteen constraints. Through the artificial bee colony process, differential search process, grid search procedure and hybrid procedure, the optimization formulation was resolved. Moreover, the constraint violation analysis and the sensitivity study were as well performed. Tiwari and Rahul [15] introduced the thermal based optimization of TRBs using Artificial-Bee-Colony (ABC) using the single objective optimization. Tiwari and Chandran [16] optimized cylindrical roller bearing design using the single−objective optimization by taking the dynamic load rating, the minimum elasto-hydrodynamic film-thickness and the maximum temperature as objective functions. Najjari and Guilbault [17] assessed a modest geometry for cylindrical roller contour. Multi-objective optimization of thermal EHL formulation was performed including edge effects through the Particle Swarm Optimization (PSA). Tiwari and Rahul [18] optimized deep-groove ball bearings (DDGBs) considering optimization of three prime objectives, i.e., the dynamic load rating, the maximum bearing temperature and the elasto-hydrodynamic minimum film thickness. Most of the above mentioned literatures show the single objective optimization of rolling element bearings. From literature survey very less publications could be found, which discusses the topic of optimization of TRBs especially to on the Dual-Objective Optimization (DOO) and the Triple-Objective Optimization (TOO). There is a need to optimize multi-objectives concurrently so as to represent the bearing as close as possible to practical situations. Hence, three objectives will be optimized simultaneously (TOO) besides performing the Single-Objective Optimization and Double objective optimization.

Genetic algorithms (GA) are an evolutionary optimization (optimization) approach that are a substitute to conventional optimization procedures, which are often gradient based. The GA are best suitable for complex non-linear models, where position of the global optimization is a challenging job. It may be possible to use the GA methodology to take up objectives, which may not be modelled as precisely through alternative methods. Therefore, GA looks to be a possibly suitable method. GA mimic the idea of result generation by randomly evolving generations of populations of solutions through a specified fitness function. These are chiefly pertinent to optimization, which are outsized, non-linear and perhaps discrete in characteristics. Also since in the present design, its variables are both continuous and discrete in nature, and with GA it can be handled relatively easier as compared to conventional gradient based optimization procedures. This probabilistic characteristic of the result is also a motive that these are not restricted by local optimization. In traditional procedure the multi-objective problem is converted to single objective using weights. These weights or parameters are varied and different combination is taken to get a range of solution on the Pareto front, from which we have to select one based on preference as to which objective is more important. Moreover, due to integer design variable and more number of constraints any combination of weighted sum may not converge to a feasible solution, so hit and trial approach

need to be done, which is time consuming. Whereas in NSGA-II, we do not need to assign weights, so we need to run the code only once to get multiple solution of the Pareto front from where a required optimized solution can be chosen. In this paper, the NSGA-II has been used to solve first three single objective functions and further simultaneously taking two objectives together, and finally taking all three objectives together. This has been done to have holistic assessment and consistency of various optimized objective functions, individually and in combination.

The rest of the work is structured as follows. Section 2 deliberates the geometrical features of TRBs. Section 3 gives the optimization expressions of TRBs, which comprises of design variables, objective expressions and constraints. Section 4 pronounces about the *multi-objective optimization* (MOO) and evolutionary procedures. Section 5 investigates the use of NSGA-II for the MOO. Section 6 deliberates the sensitivity investigation. Section 7 is devoted to argument on results, which are obtained in section 5. Last Section 8 accomplishes deductions of the present analysis.

2. Geometrical aspects of TRBs

Generally, TRBs contains four components, (1) cup (outer raceway), (2) cone (inner raceway) with guide flanges, (3) tapered rollers and (4) cage (space retainer). These parts are somewhat different from the remaining roller bearings. The set of rollers is contained by cage on the cone with guide flanges as a single unit. Figure 1 shows a section view of a TRB without cage. Theoretically, the extensions of all the contact lines between tapered rollers and the inner or outer raceway should intersect at one common point on the bearing axis for pure rolling condition to prevail. The nominal contact angle of the bearings is in the range 10° to 30° [19]. Larger contact angles are used to carry heavy axial loads. Due to the presence of difference in the inner and outer ring contact angles, there is a force component that drives the rollers against the guide flange.

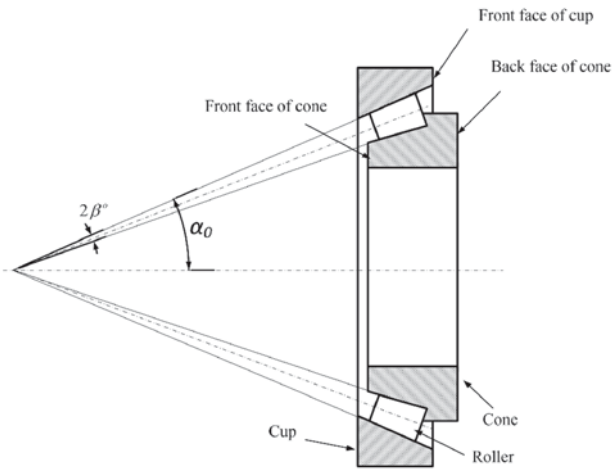

Figure 1. A section view of a tapered roller bearing.

TRBs are identified by utilizing the basic periphery sizes, like the exterior diameter (D), bore diameter (d), width of cup (C), width of cone (B) and total width of bearing (T). Figure 2 shows the single-row TRB nomenclature with specification of peripheral geometries as per bearing standard [20]. Apart from the basic dimensions, remaining are used to convey the whole geometry of the TRB.

3. Problem formulation for TRB design

Main motive of the present design is to obtain dimensions of interior geometrical variables of TRBs (i.e., the pitch diameter, roller diameter, number of rollers, operative roller length and contact angle) under a specified TRB standard periphery dimensions (exterior diameter, bore diameter, width of cup, width of cone and total width) by using optimization methodology. With this, improved performance and lifespan of the bearing than standard TRBs is expected. Common constrained optimization formulation is expressed as,

$$\begin{aligned} &\text{Objectives}: \quad \text{Minimize or Maximize} \quad f_m(\mathbf{x}) \\ &m = 1, 2, \cdots, \mathrm{M} \\ &\text{Constraints}: \quad \text{Subjected to}: \\ &\qquad g_j(\mathbf{x}) \geq 0, \qquad j = 1, 2, \cdots, J \end{aligned} \tag{1}$$

$$h_k(\mathbf{x}) = 0, \qquad k = 1, 2, \cdots, K \tag{2}$$

$$\begin{aligned} &\text{Variable bounds}: \quad x_l^{(L)} \leq x_l \leq x_l^{(U)}, \quad x_l \in \mathbf{x}, \\ &l = 1, 2, \cdots, L \end{aligned} \tag{3}$$

Nomenclature is provided for all variables. In following subsections. Now the design variables, objectives and constraints for the TRB optimization are described.

3.1 *Design variables*

The commonly sovereign design parameters that is to be found by the optimization are called design variables. The design variable vector, x, utilised in the optimization of TRB is

$$\mathbf{x} = \lfloor D_m \quad D_r \quad l_e \quad \alpha_o \quad Z \quad K_{D_{\min}} \quad K_{D_{\max}} \quad \varepsilon \quad e \quad \beta \quad \zeta \rfloor^T \tag{4}$$

Five design variables D_m, D_r, Z, l_e and α_o signify the interior geometry of TRBs (see figure 2) and additional six variables are utilised in constraints to provide the TRB optimization a feasible design space. Herein values of $K_{D_{min}}, K_{D_{max}}, \varepsilon, e, \beta$ and ζ are obtained through the optimization instead of taking them as fixed values. These

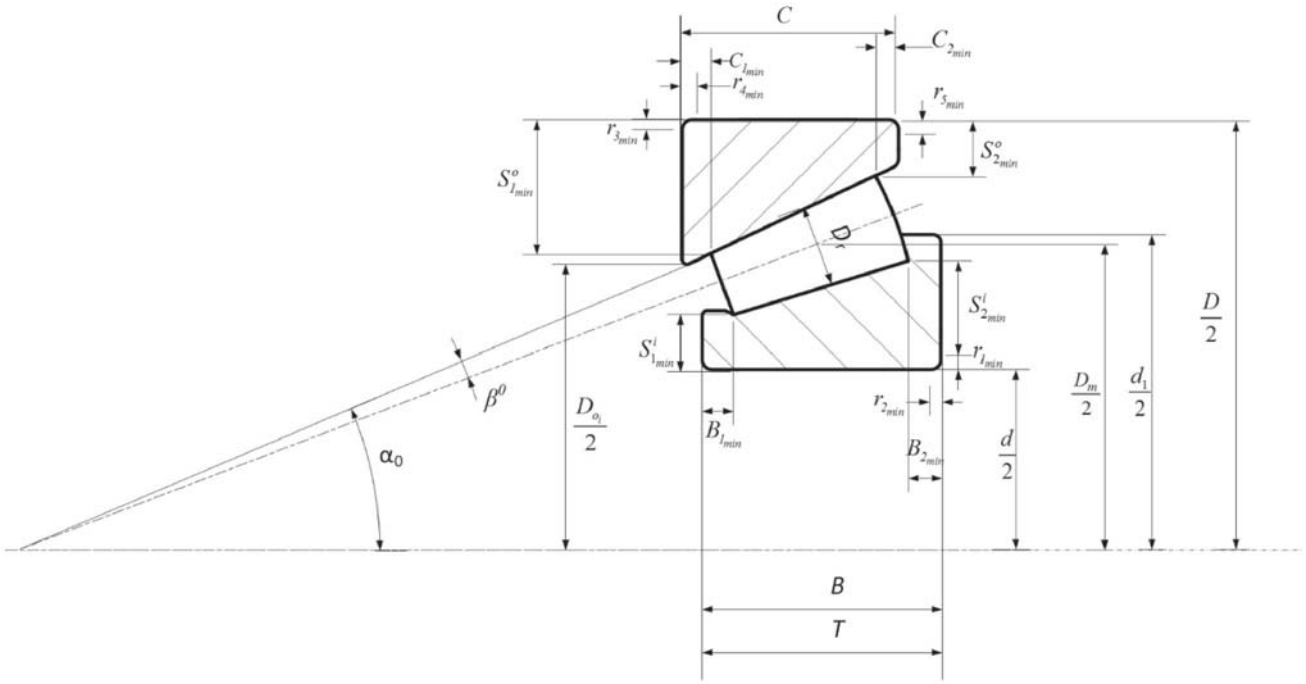

Figure 2. A sectional view of a tapered roller bearing with the cup, cone and roller.

terms do not directly represent the bearing internal geometry rather they are used only in constraints that gives the bearing a feasible design space. In this work, these parameters are taken as variables same as other design variables. Conventionally these are being used fixed values for all bearings but in the present case they will be different for different bearings. In fact, a feasible range of these variables are given during its optimization along with other geometric design variables.

3.2 *Objective function*

The expressions that are to be optimized are named as objectives. The objective function may be of the minimization kind or the maximization kind. The minimization of $f(x)$ could be changed to maximization of "- $f(x)$" or "1/$f(x)$" and likewise to transform from the maximization to the minimization, this norm is termed as the *duality norm*. Often it is obligatory to optimize multiple objectives that is termed as the multiple-objective optimization. In the current optimization, three objectives, that are the dynamic capacity (C_d), the minimum elasto-hydrodynamic lubrication film-thickness (h_{min}) and maximum bearing temperature (T_{max}), are planned to optimize. These objectives will be described as follows.

3.2a *Dynamic load rating:* The dynamic load rating (or dynamic capacity) is termed as the fixed radial force that a collection of seemingly alike bearings can tolerate for a rating life of one million revolutions of the interior ring for a static force and the fixed exterior ring. Irrespective of type of external loading on the TRB, like the preload, axial load, radial load and couple, the dynamic load rating ensures final stresses at contact lines are within acceptable plastic deformation, if any. The equation for dynamic load rating of TRB is expressed as [21]

$$C_d = b_m f_c (i l_e \cos\alpha_o)^{7/9} Z^{3/4} D_r^{29/27} \tag{5}$$

with

$$f_c = 207.9 \lambda v \gamma^{2/9} \frac{(1-\gamma)^{29/27}}{(1+\gamma)^{1/4}} \left[1 + \left\{1.04 \left(\frac{1-\gamma}{1+\gamma}\right)^{143/108}\right\}^{9/2}\right]^{-2/9} \tag{6}$$

and

$$\gamma = \frac{D_{r_{mean}}}{D_m} \cos\alpha_o; \qquad D_{r_{mean}} = \frac{1}{2}(D_{r_{LL}} + D_{r_{UL}}); \tag{7}$$

Usually, the life of bearing denotes to its fatigue life that is stated as the rating life. Aggregate sum of bearing rotations or the total duration in hours at a specified fixed speed that the bearing is accomplished before an initial mark of fatigue appears at exterior rig races of bearing is termed the rating life. The L_{10} life of the bearing subjected the equivalent radial force is expressed by

$$L_{10} = 10^6 \left(\frac{C_d}{P}\right)^{10/3} \text{ rev.} \tag{8}$$

It is apparent from Eq. (8) that the dynamic load rating of bearing and it's the life are related. Hence, one of the objective has been considered as the maximization of dynamic load rating. Observing Eq. (5), one can conclude that by the optimization, variables l_e, Z and D_r are to be maximized and α_o is to be minimized to obtain the highest value of dynamic capacity. However, constraints limit the maximum values of parameters. Moreover, while rollers with the highest diameter are to be considered then number of rollers would be fewer in a specified space. Hence based on above discussions, the primary objective has been considered as the maximization of dynamic load rating, as

$$f_1(\mathbf{x}) = \max\{C_d(\mathbf{x})\} \tag{9}$$

3.2b *Elasto-hydrodynamic minimum film-thickness:* The elasto-hydrodynamic minimum film-thickness is another objective function taken for the optimization. The wear is an important means of failure of rolling or sliding in machine elements. To decrease the wear by evading metal-to-metal contact between rollers and raceways, frequently the lubrication is put in bearings. Rolling elements experience distortion owing to the occurrence of confined extraordinary contact pressures (i.e., the Hertzian contact pressure) in bearings. To analyse the lubricating performance of the oil-film between two elastic elements, which are in comparative rolling or a rolling supplemented by the sliding, the theory of EHL was suggested. By means of the EHL theory, the minimum film thickness can be obtained based on interior geometries and operating parameters. For the interior and exterior rings, the minimum film thicknesses for are expressed as per [19]

$$(h_{min})_{inner,outer} = \frac{3530 U_{i,o}^{0.7} G^{0.54}}{q_{i,o}^{0.13}} R_{e_{i,o}} \tag{10}$$

where

$$U_{i,o} = \frac{\eta_0 u_{i,o}}{2E' R_{e_{i,o}}}; \qquad G = \alpha_p E'; \qquad q_{i,o} = \frac{Q_{i,o}}{l_e E' R_{e_{i,o}}};$$
$$R_{e_{i,o}} = \frac{D_r}{2}(1 \mp \gamma_{i,o}); \tag{11}$$

$$E' = \frac{E}{1-\upsilon^2}; \qquad Q_{i,o} = \frac{5P}{Z\cos\alpha_o};$$
$$\gamma_i = \frac{D_r \cos(\alpha_o - 2\beta^\circ)}{D_m}; \qquad \gamma_o = \frac{D_r \cos\alpha_o}{D_m} \tag{12}$$

$$u_i = \frac{D_m}{2}[(1-\gamma_i)(\omega_0 - \omega_m) + \gamma_i \omega_r];$$
$$u_o = \frac{D_m}{2}[(1+\gamma_o)\omega_m + \gamma_o \omega_r]; \tag{13}$$

$$\omega_m = \frac{\pi}{60}[n_o(1-\gamma_o)]; \qquad \omega_r = \frac{\omega_m D_m}{D_r}[n_o(1-\gamma_i)];$$
$$\omega_o = \frac{2\pi n_o}{60}; \tag{14}$$

While the minimum film-thickness grows, the wear in the bearing decreases. This is due to the fact that it evades the metal-to-metal contact between rollers and rings. So, the additional objective expression selected is

$$f_2(\mathbf{x}) = \max\{h_{min}(\mathbf{x})\} \tag{15}$$

with

$$h_{min}(\mathbf{x}) = \min[\{h_{min}(\mathbf{x})\}_{inner}, \{h_{min}(\mathbf{x})\}_{outer}] \tag{16}$$

3.2c *Maximum bearing temperature:* In bearings, part of the rotational energy converts into heat due to the friction. As the bearing temperature plays a vital role in selecting the type of lubricant and the material of the bearing, it is important to know the different temperatures of the bearing assembly. As the temperature increases, lubricant may not serve the purpose it is intended to and the life of bearing also gets affected. Utilizing the finite difference expressions in two stages [22], contact point temperatures have been obtained. The lubricant temperature at different nodes (see figure 3) has been obtained with the help of the system of linear equations that are given in table 1. The maximum temperature in the bearing typically arises at the interior ring and the roller interface (refer figure 4). The inner ring-roller contact temperature (T_{max}) is obtained by solving equations in table 2. In tables 1 and table 2 for all parameters SI units are used. In this analysis, the variation of dynamic viscosity of lubricant with the lubricant

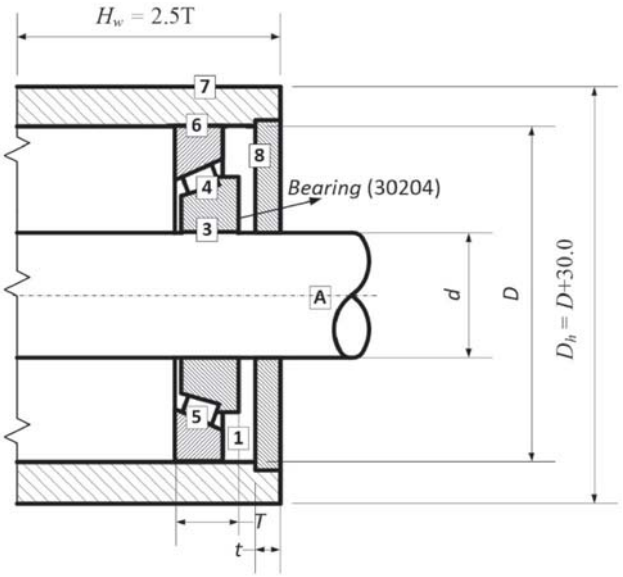

Figure 3. The housing and the bearing with various Temperature nodes.

Table 1. For the bearing and its frame the governing equations for its thermal stability.

Nodes	Thermal balance equations
1	$0.0288k_o\,\mathrm{Pr}^{1/3}\left[\sqrt{(u_i/v_o d_i)}A_{14}(T_{l_1}-T_{l_4})+\sqrt{u_o/v_o d_o}A_{15}(T_{l_1}-T_{l_5})+\sqrt{(u_s/v_o D)}A_{18}(T_{l_1}-T_{l_8})+\sqrt{(u_s/v_o)}DA_{13}(T_{l_1}-T_{l_3})\right]=0$
	$A_{14}=\pi d_i T;A_{15}=\pi d_o T;A_{18}=\pi(D^2-d^2)/4+\pi d_o(H_w-T);A_{13}=\pi d(H_w-T);d_o=D_m+D_r\cos(\alpha_o-\beta^\circ);d_i=D_m-D_r\cos(\alpha_o-\beta^\circ)$
2	$kA_{2a}(T_{l_2}-T_a)/\ell_{2a}+kA_{23}(T_{l_2}-T_{l_3})/\ell_{23}=0\;A_{2a}=\pi d^2/4;A_{23}=dH_w;\ell_{2a}=T/2;\ell_{23}=d/2$
3	$kA_{32}(T_{l_3}-T_{l_2})/\ell_{32}+2\pi k\varpi_{34}(T_{l_3}-T_{l_4})/\ln(d_i/d)+0.0288k_o\,\mathrm{Pr}^{1/3}\sqrt{(u_s/v_o D)}A_{31}(T_{l_3}-T_{l_1})=0$
	$A_{32}=A_{23};\varpi_{34}=T;\ell_{32}=\ell_{23};A_{31}=A_{13}$
4	$0.0288k_o\,\mathrm{Pr}^{1/3}\sqrt{(u_i/v_o d_i)}A_{41}(T_{l_4}-T_{l_1})+2\pi k\varpi_{43}(T_{l_4}-T_{l_3})/\ln(d_i/d)-H_{f_{race(i)}}=0;$
	$H_{f_{race(i)}}=1.047\times10^{-1}\times n_o\times\left(M_{race(i)}+M_{rib}\right)+H_{f_v}/2H_{f_v}=1.047\times10^{-1}\times n_o\times M_v;M_{race(i)}=Zd_iM_o/2D_r;M_o=\left(1.76\times10^2/(1+0.29L_o^{0.78})\right)(GU_o)^{0.658}W^{0.31}lR_{e_o}^2/\alpha_p$ ([26])
	$M_v=10^{-10}f_o(v_o n)^{2/3}D_m^3;M_{rib}=h_f\mu_o\cos\beta^\circ F_a\exp\left(-1.8\lambda_r^{1.2}\right);A_{41}=A_{14};\varpi_{43}=T$
5	$0.0288k_o\,\mathrm{Pr}^{1/3}\sqrt{(u_o/v_o d_o)}A_{51}(T_{l_5}-T_{l_1})-H_{f_{race(o)}}+2\pi k\varpi_{56}(T_{l_5}-T_{l_6})/\ln(D/d_o)=0;A_{51}=A_{15};$
	$\varpi_{56}=TH_{f_{race(o)}}=1.047\times10^{-1}\times n_o\times M_{race(o)}+H_{f_v}/2;M_{race(o)}=\frac{Zd_o}{2D_r}M_i;M_i=\left(1.76\times10^2/(1+0.29L_i^{0.78})\right)(GU_i)^{0.658}W^{0.31}R_{e_i}^2l/\alpha_p$([26])
6	$2\pi k\varpi_{65}(T_{l_6}-T_{l_5})/\ln(D/d_o)+2\pi k\varpi_{67}(T_{l_6}-T_{l_7})/\ln(D_h/d)=0;\;\varpi_{65}=T;\;\varpi_{67}=T$
7	$h_{v_{7a}}A_{7a}(T_{l_7}-T_a)+h_{r_{7a}}A_{7a}(T_{l_7}-T_a)+\frac{2\pi k\varpi_{76}(T_{l_7}-T_{l_6})}{\ln(D_h/D)}+\frac{A_{78}(T_{l_7}-T_{l_8})}{\ell_{78}}=0;A_{7a}=\pi D_h(T+0.25D_h);\varpi_{76}=T;A_{78}=\pi(D^2-d^2)/4;\ell_{78}=t$
8	$0.0288k_o\,\mathrm{Pr}^{1/3}\sqrt{(u_s/v_o D)}A_{81}(T_{l_8}-T_{l_1})+kA_{87}(T_{l_8}-T_{l_7})/\ell_{87}=0;\;A_{81}=A_{18}\;\ell_{87}=t;\;A_{87}=A_{78}$

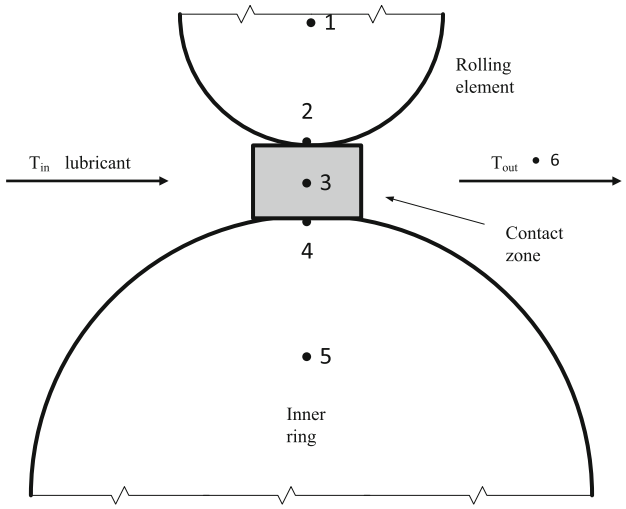

Figure 4. Roller-lubricant-interior ring temperature nodes.

temperature has been considered. Taking into the account of above mentioned points, the maximization of ($-T_{max}$) has taken as the third objective for optimization.

$$f_3(\mathbf{X}) = \max(-T_{max}) \tag{17}$$

3.3 *Optimization related constraints*

Constraints are defined as the limits executed on the selection of design variables. Equality constraints and inequality constraints are two kinds of constraints generally encountered. Total twenty-eight diverse constraints are formulated and explained now. For the uniqueness, all inequality constraints are denoted as bigger than or alike kinds (refer table 3). For one design variable or combination of design variables, more than one constraint has been developed. It should be noted that some of constraints may be redundant in some size of bearings but may be relevant for other. So the intention in developing these constraints is that all possible feasible constraints to be included so that the design is robust against all odds. The following constraints are formulated based on internal geometric properties obtained from the trigonometric relations. Using trigonometric relations, all other internal geometries of the bearing can be related with boundary dimensions and these relations include basic design variables (see Appendix A).

Constraints 1 and 2: In view of the space for the chamfering radius on both the interior and exterior rings, the choice of pitch diameter could be attained such that it should lie between the bearing exterior and bore diameters. *Constraints* 3 and 4: With the strength and geometrical deliberations the range for roller diameter is attained [13]. *Constraints* 5 and 6: Constraints on the effective roller length are provided from the fact that the roller length is never less than its diameter and should not protrude from both faces of the cup and to take care of cages. *Constraints* 7 and 8: The higher bound of number of rollers is acquired from the higher bound of pitch diameter and the lower bound of roller diameter, and other way round to get the lower bound. *Constraints* 9 and 10: Unknown constraint variables $K_{D_{min}}$ and $K_{D_{max}}$ gives alternative set of constraints for the roller diameter. These and some more that follows have been considered as design variables as discussed in section 3.1. *Constraints* 11 and 12: To confirm movement of the bearing, the pitch diameter minus the average diameter of TRB should be below a unknown variable, e. *Constraint* 13: The depth of the bearing ring at the exterior raceway bottom should be more than εD_r, where ε is the new constraint factor. *Constraint* 14: From given peripheral

Table 2. Thermal equilibrium equations for the inner ring and roller contact.

Nodes	Thermal balance equations
1	$kA_{21}(T_2 - T_1)/L_{21} + (h_v)_{61}A_{61}(T_6 - T_1) = 0;\ A_{21} = \text{rmsofarea} = 0.5774D_r l;$ $A_{61} = \pi D_r l/4; L_{21} = D_r/2$
2	$kA_{12}(T_1 - T_2)/L_{12} + k_o A_{32}(T_3 - T_2)/L_{32} = 0;$ $A_{12} = A_{12}; A_{32} = 2b_i l; b_{i,o} = 3.35 \times 10^{-3}\sqrt{(Q_{i,o}D_r(1 \mp \gamma)/2l)};\ L_{32} = h_{inner,outer}/2$
3	$k_o A_{23}(T_2 - T_3)/L_{23} + k_o A_{43}(T_4 - T_3)/L_{43} + H_{gen} - wC_p(T_6 - T_{in}) = 0$ $H_{gen} = H_{f_{race(i)}}/Z;\ w = 5.879 \times 10^{-8}\mu Q_{i,o}D_m n_o/2Z; A_{23} = A_{32}; A_{43} = A_{32}; L_{23} = L_{32};\ L_{23} = L_{32}$
4	$k_o A_{34}(T_3 - T_4)/L_{34} + kA_{54}(T_5 - T_4)/L_{54} = 0;$ $A_{34} = A_{32}; A_{54} = \text{rmsofarea} = (2\pi T/Z)\sqrt{(r_o^2 + r_i^2 + r_o r_i)/3};\ L_{34} = L_{43};\ L_{54} = (d_i - d)/4$
5	$k_b A_{45}(T_4 - T_5)/L_{45} + (h_v)_{65}A_{65}(T_6 - T_5) = 0; A_{45} = A_{54};\ L_{45} = L_{54};$ $A_{65} = \pi d_i T/2Z$
6	$(h_v)_{61}A_{61}(T_6 - T_1) + (h_v)_{65}A_{65}(T_6 - T_5) + wC_p(T_6 - T_{in}) = 0;$ $(h_v)_{65,61} = 0.11(0.5Re_o + Gr_o Pr)^{0.35}k_o/d_o;\ A_{61} = \pi D_r l/4$

Table 3. Constraints for design variables.

Constraint Number	Range of the variable and constraints	
1 & 2	$(d+2r_{1_{min}}) \le D_m \le (D-2r_{3_{min}})$	$g_1(\mathbf{X}) : D_m - (d+2r_{1_{min}}) \ge 0$ $g_2(\mathbf{X}) : (D-2r_{3_{\min}}) - D_m \ge 0$
3 & 4	$D_{r_{LL}} \le D_r \le D_{r_{UL}}$ with $D_{r_{LL}} = 212.43(Q_{\max})^{0.5}/\sigma_{c_{\max}}$ and $D_{r_{UL}} = \frac{1}{2}\left\{\frac{(D-2r_{3_{min}})-(d+2r_{1_{min}})}{\cos\alpha_o}\right\}$	$g_3(\mathbf{X}) : D_r - D_{r_{LL}} \ge 0$ $g_4(\mathbf{X}) : D_{r_{UL}} - D_r \ge 0$
5 & 6	$D_{r_{LL}} \le l_e \le l_{e_{UL}}$	$g_5(\mathbf{X}) : l_e - D_{r_{LL}} \ge 0$ $g_6(\mathbf{X}) : \frac{(C-r_{5_{min}}-r_{4_{min}})}{\cos\alpha_o} - l_e \ge 0$
7 & 8	$\frac{\pi(d+2r_{1_{min}})}{D_{r_{UL}}} \le Z \le \frac{\pi(D-2r_{3_{min}})}{D_{r_{LL}}}$ with $0.3 \le K_{D_{min}} \le 0.4$ [8] $0.5 \le K_{D_{max}} \le 0.6$ [8]	$g_7(\mathbf{X}) : Z - \frac{\pi(d+2r_{1_{min}})}{D_{r_{UL}}} \ge 0$ $g_8(\mathbf{X}) : \frac{\pi(D-2r_{3_{min}})}{D_{r_{LL}}} - Z \ge 0$
9 & 10	$K_{D_{\min}}\left[\frac{(D-d)}{2\cos\alpha_o}\right] \le D_r \le K_{D_{\max}}\left[\frac{(D-d)}{2\cos\alpha_o}\right]$	$g_9(\mathbf{X}) : D_r - K_{D_{\min}}\left[\frac{(D-d)}{2\cos\alpha_o}\right] \ge 0$ $g_{10}(\mathbf{X}) : K_{D_{\max}}\left[\frac{(D-d)}{2\cos\alpha_o}\right] - D_r \ge 0$
11 & 12	$g_{11}(\mathbf{X}) : D_m - (0.5-e)(D+d) \ge 0;$	$g_{12}(\mathbf{X}) : (0.5+e)(D+d) - D_m \ge 0$ with $0.01 \le e \le 0.07$[8]
13	$0.5(D-D_m-D_r)sec\alpha_o - \varepsilon D_r \ge 0$	$g_{13}(\mathbf{X})$: with $0.4 \le \varepsilon \le 0.5$[8]
14	$g_{14}(\mathbf{X}) : S^o_{2_{\min}} - \left\{\frac{D}{2} - \left(\frac{D_{o_{inner}}}{2} + C\tan\alpha\right)\right\} \ge 0$	
15 to 17	$g_{15}(\mathbf{X}) : S^i_{1_{min}} - S^o_{2_{min}} \ge 0;$	$g_{16}(\mathbf{X}) : C_{2_{min}} - r_{5_{min}} \ge 0$; $g_{16}(\mathbf{X}) : C_{1_{min}} - r_{4_{min}} \ge 0$
18 to 20	$g_{18}(\mathbf{X}) : B_{2_{min}} - r_{2_{min}} \ge 0;$	$g_{19}(\mathbf{X}) : B_{1_{min}} - r_{5_{min}} \ge 0$; $g_{20}(\mathbf{X}) : B_{2_{min}} - B_{1_{min}} \ge 0$
21	$g_{21}(\mathbf{X}) : C_{1_{min}} - C_{2_{min}} \ge 0$	
22	$g_{22}(\mathbf{X}) : \beta C\sec(\alpha_o) - l_e \ge 0$with$0.8 \le \beta \le 0.95$[8]	
23 to 25	$g_{23}(\mathbf{X}) : \left(\frac{D}{2} - S^o_{1_{min}}\right) - \frac{D_{o_{inner}}}{2} \ge 0$; $g_{24}(\mathbf{X}) : \sigma_y - \sigma_{f_{max}} \ge 0;$	$g_{25}(\mathbf{X}) : \sigma_{safe} - \sigma^l_{max} \ge 0$
26	$g_{26}(\mathbf{X}) : 2\pi - 2Z\sin^{-1}(D_r\cos\alpha_o/D_m) \ge Z\pi/180$	
27	$g_{27}(\mathbf{X}) : Z(2D_r/D_m + \pi/180) \ge 2\pi - 2D_r/D_m$	
28	$g_{28}(\mathbf{X}) : S^o_{2\min} \ge [r_{5_{min}} + 1.0 + C_{2_{min}}\tan(\alpha_o)]$	

sizes of the bearing, a constraint on the $S^o_{2_{min}}$ has imposed [23]. *Constraint* 15: In the TRB cone gets more stresses than the cup due to its convex curvature. Keeping that in mind, a constrained has been obtained such that the minimum thickness of the cone $S^i_{1_{min}}$ is more than the minimum thickness of the cup, $S^o_{2_{min}}$. *Constraint* 16: The least width of the front-face of the cup, $C_{2_{min}}$, should be greater as compared to the least value of $r_{5_{min}}$ to evade the interaction of the roller with the curved-end of the front-face of the cup and to evade projection of the big-end of the roller. *Constraint* 17: A constraint on the $C_{1_{min}}$ is provided to include chamfering to faces of the cup and also to keep away the bends of the small end of the roller, from the back-face chamfer of the cup. *Constraint* 18: A constraint on $B_{2_{min}}$derived so that the big end of the roller should be far from the chamfer of the back-face of the cone. *Constraint* 19: $B_{1_{min}}$ has a constraint in order to keep the bend of the small end of the roller from the front-face of the cone. *Constraint* 20: $B_{2_{min}}$ should be greater than $B_{1_{min}}$ for the reason that the major lip of the cone is the risky part that bears the longitudinal constituent of loads, while the minor lip of the cone merely holds the tapered rollers on the cone. *Constraint* 21: Generally, in TRBs, the width of the back-face of the cup should be greater as compared to the width of the front-face of the cup. *Constraint* 22: Another constraint on the effective length of the roller has been provided to limit the maximum value of it, which includes unknown constraint factor β. *Constraint* 23: The minor end of the roller should not project from the cup. *Constraint* 24: The extreme principal stress at the flange of the cone owing to the flange force should be inside the yield strength of the material of the flange. *Constraint* 25: In rolling bearings, enormous extent of loads is focused at a moderately lesser contact area, ensuing in excessive contact stresses, which results to minor extent of perpetual distortion. The stresses thus produced should be within 4000 MPa [21]. The 30% ofC_d is considered as the equivalent radial load for calculating the two stress constraints 24 and 25. But for optimizing h_{min} and T_{max}, an equivalent radial load has taken as 10% of C_d, since the actual bearing will not be subjected to this much of very high loads. *Constraint* 27: A constraint on the number of rollers is achieved in view of a standard angular gap of 1 degree between two rollers to safeguard smooth movements of rollers. *Constraint* 28: To avoid the sharp corner at the cup big-end $S^o_{1_{min}}$ should be greater than

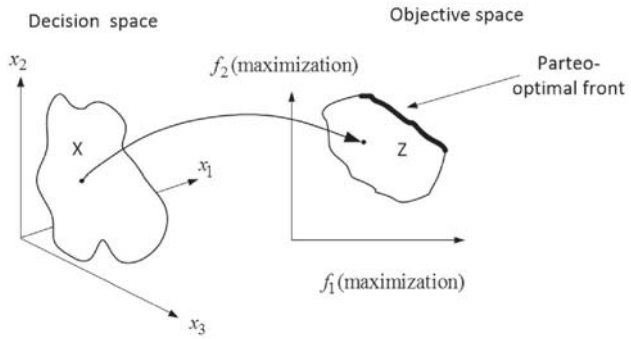

Figure 5. Depiction of the choice space and the matching target space with the Pareto-optimal front.

the radius of the cup $r_{5_{min}}$, and additional it is provided with a land of minimum 1 mm.

4. Multi-objective optimisation and evolutionary algorithm

Optimization is the enactment of attaining finest results beneath specified conditions. Typically, the standard optimization formulation comprises of design variables,

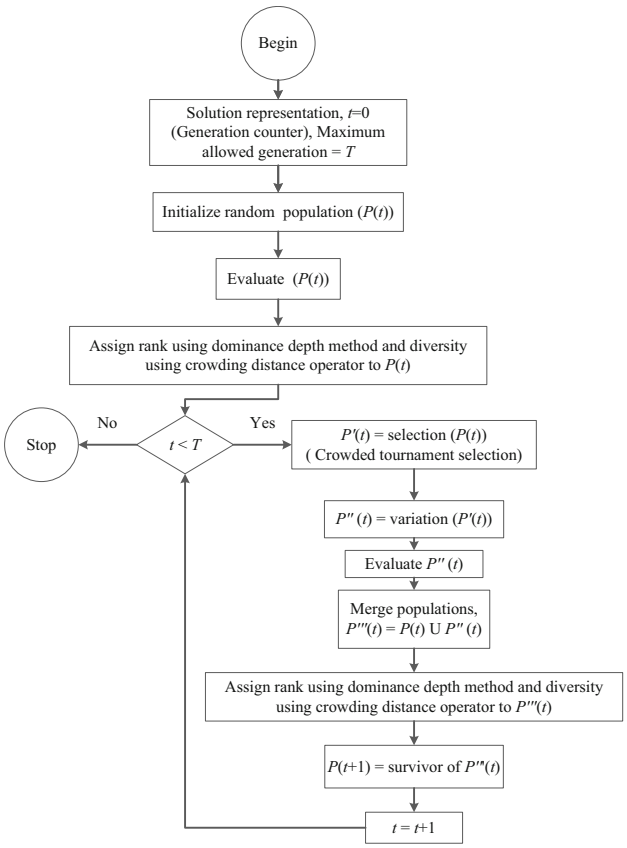

Figure 6. Flow chart of the NSGA-II algorithm.

Table 4. Bearing material parameters and additional physical constants.

Property	Value	Property	Value
σ_{safe}	4000 MPa	b_m	1.1 [27]
σ_y	600 MPa	v	1.2 [21]
n_o	6200 rpm	λ	0.65
E	210000 MPa	υ	0.3
Th	3 mm	ε_h	0.03
k_b	47 W/mK	I	1

Table 5. Lubricant data of grease at 100°C [28].

Property	Value	Property	Value
α_p	1.15e-8 m^2/N	β_c	0.00065 1/K
β_o	0.0156 1/K	C_p	2130 J/Kg-K
k_o	0.1 W/mK	η_o	0.00162 Pa-S
v_o	1.9e-6 m^2/S	ρ	852.3 Kg/m^3

Table 6. Air properties at ambient temperature 40°C.

Property	Value	Property	Value
v_a	23.06e-6 m^2/S	Pr_a	0.7
k_a	0.0314 W/mK		

objectives and constraints. Optimization problems concerning two or more objectives are recognised as *Multi-Objective Optimization Problem* (MOOP). Often real life optimization problems include numerous objectives. Essential modifications of the MOOP as compared with the SOO problem are (i) manifold of optimized results as compared to merely single, (ii) two (or more) objectives rather than one single, obtaining group of results nearby to POF and varied results, and (iii) handling with two (or more) exploration spaces as an alternative of single, i.e., the choice space and the objective space.

Objectives in the MOOP are usually conflicting among themselves, i.e., the improvement in one objective results in the harm in however in one of other objectives. These *trade-off fronts* are termed as *Pareto fronts*. Hence, a single result that concurrently optimize entire objectives does not occur. Instead, the finest trade-off results, termed *Pareto-optimal fronts* (POFs), are utilized for selection of choice in getting an appropriate optimized point. Hence, it is favoured to have results that are on or close by POFs.

Figure 5 depicts the *design variable space* and conforming *objective space*. For every result vector x in the choice space, there occurs a point in the objective space, z. The transformation occurs between *l*-dimensional result vector and an *m*-dimensional objective vector. The MOO is

Table 7. Standard TRB dimensions utilised for the TRB design [20, 29].

	Standard periphery sizes (mm)					Standard internal and chamfering dimensions (mm)							
Bearing no.	D	d	C	B	T	d_1	$D_{o_{inner}}$	$r_{1_{min}}$	$r_{2_{min}}$	$r_{3_{min}}$	$r_{4_{min}}$	$r_{5_{min}}$	C_d (KN)
30204	47	20	12	14	15.25	33.20	37.304	1.0	1.0	1.0	1.0	0.5	27.5
30205	52	25	13	15	16.25	37.40	41.135	1.0	1.0	1.0	1.0	0.5	30.8
32205	52	25	15	18	19.25	40.20	37.555	1.0	1.0	1.0	1.0	0.5	35.8
322/28	58	28	16	19	20.25	43.90	42.436	1.0	1.0	1.0	1.0	0.5	41.8
30206	62	30	14	16	17.25	44.60	49.990	1.0	1.0	1.0	1.0	0.5	40.2
32206	62	30	17	20	21.25	45.20	48.982	1.0	1.0	1.0	1.0	0.5	50.1
30306	72	30	16	19	20.75	48.40	58.287	1.5	1.5	1.5	1.5	0.4	56.1
32207	72	35	19	23	24.75	52.40	57.087	1.5	1.5	1.5	1.5	0.5	66.0
32208	80	40	19	23	24.75	58.40	64.715	1.5	1.5	1.5	1.5	0.5	74.8

often terms as a *vector optimization* since a vector of objectives, rather than a single objective, is optimized. When entire objectives and constraints are linear, the subsequent MOOP is termed as a multi-objective linear formulation. However, often actual formulations are of non-linear kind. The current optimization formulation of TRBs is a non-linear one.

In the MOOP to match two results the *notion of domination* is utilised to verify if one result dictates the other or not. A result vector x is supposed to dictates (more optimized) a new result vector y, when the result vector x is no inferior compared to y in entire objectives and x is sternly superior compared to y in at least one objective. In view of entire objectives are of the maximization kind, the supremacy of x is expressed as

$$\mathbf{x} \succ \mathbf{y} :\Leftrightarrow \{f_m(\mathbf{x}) \not< f_m(\mathbf{y}) \forall m \quad \text{and} \quad f_m(\mathbf{x}) > f_m(\mathbf{y}) \text{ for at least one } m\} \tag{18}$$

Herein, x$\succ$y represents supremacy of x over y (for further mathematical symbols see Nomenclatures). The group of non-dominated results in a confined choice space is termed as the non-dominated front. The universal non-dominated result group is the *Pareto-optimal group*. Hence, it can be concluded that, all POFs are non-dominated however entire non-dominated fronts are not POFs.

Multi-objective optimization procedures can be characterised into *traditional procedures* and *evolutionary procedures*. Additionally, as per Cohon [24], traditional procedures can be sub-categorised as the *generating* and *preference-based procedures*. In generating procedures, a handful of non-dominated results are produced for the handler, who subsequently elects single result from the acquired non-dominated results. No previous information regarding individual objective is compulsory. While preference centred procedures utilise a few recognised inclinations for individually objective. Often traditional procedures transform the MOOP into a SOOP through some weights. Complications of traditional procedures are: essential to execute the single objective optimization numerous epochs and plenty of problem information is compulsory. Evolutionary Algorithms (EA) imitates natural evolutionary philosophies to establish the exploration and optimization techniques. The representative characteristic of EAs is obtaining and preserving numerous results in a single recreation run. When traditional approach is used than for each set of weights the algorithm has to go through local optimal point and infeasible regions to reach to the Pareto front. Again when we start with new weights all the information about the local optimal points and infeasible regions are lost and the algorithm needs to learn all over again. Evolutionary algorithm deals with a population rather than a point, if any member of the population reaches the Pareto front due to mutation or crossover, it will definitely generate more copies in tournament selection operator. When other members of solution get crossed with copies of this better solution they will quickly come closer to the Pareto front. This is the parallelism in population based methods, which we do not have in classical methods

Table 8. Bounds of design variables for TRB model 30204.

Parameter	Value	Parameter	Value
D_m	22 - 45 mm	$K_{D_{min}}$	0.30 - 0.40
D_r	2.737 - 11.852 mm	$K_{D_{max}}$	0.50 - 0.60
Z	6 - 50	ε	0.40 - 0.50
l_e	2.737 - 10.821 mm	E	0.01 - 0.07
α_o	10° - 30°	β	0.80 - 0.95
		ζ	0.125 - 0.250

Table 9. GA variables bounds and preferred value.

GA Variables	Bounds	Preferred value
Crossover probability	0.70-0.90	0.85
Mutation probability	0.1-0.2	0.1
Crossover distribution index	1-100	10
Mutation distribution index	1-100	20
Random seed	0-1	0.1

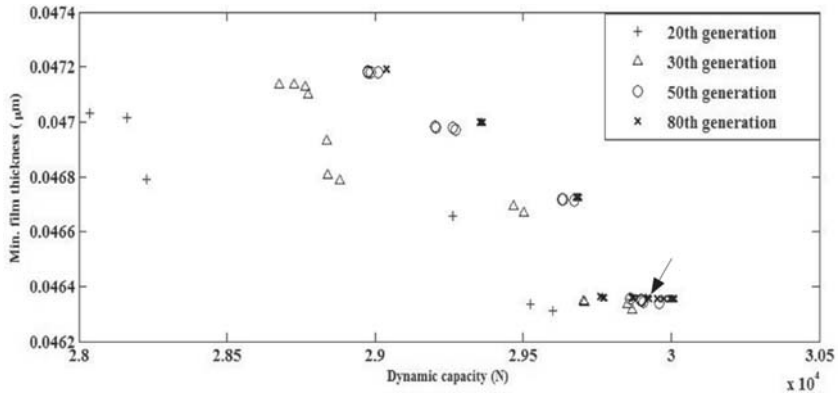

Figure 7. Convergence of $C_d - h_{min}$ front with the generation for the TRB 30204.

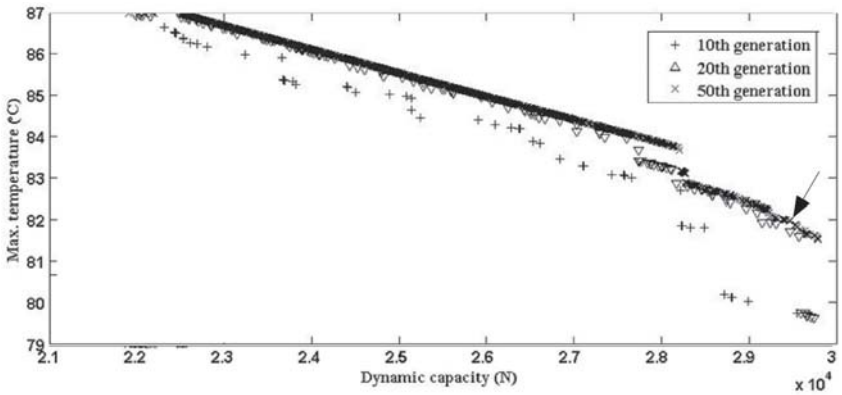

Figure 8. Convergence of $C_d - T_{max}$ front with the generation for the TRB 30204.

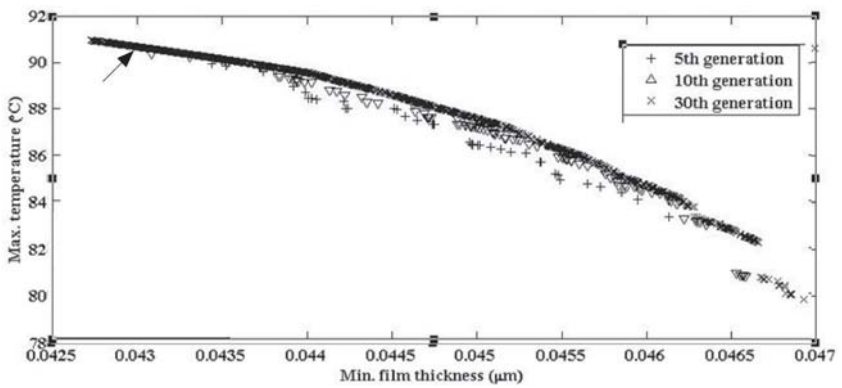

Figure 9. Convergence of $h_{min} - T_{max}$ front with the generation for the TRB 30204.

because there is no memory. This implicit parallelism makes NSGA-II superior to weighted sum approach computationally. Moreover, if the Pareto front is non-convex NSGA-II will generate more points on Pareto-optimal front than classical weighted sum approach [25].

As illustration for the present case, in weighted sum approach to generate 50 Pareto optimal fronts we have to select 50 different sets of weights and run the algorithm 50 times. In weighted sum approach the multi-objective problem gets converted into single objective problem. For a

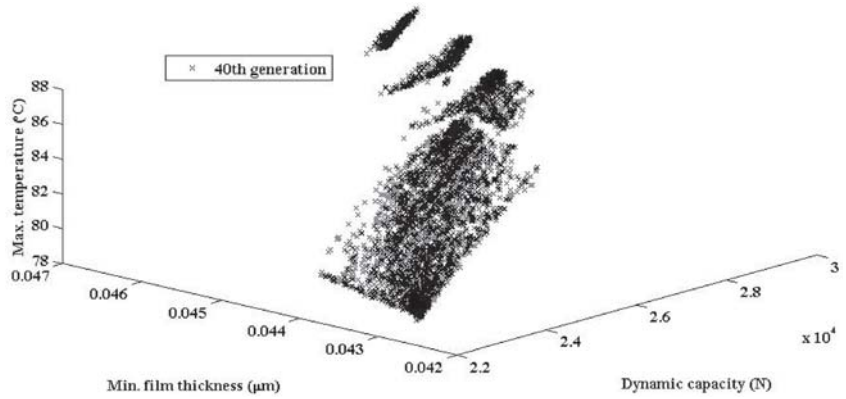

Figure 10. The POS obtained by MOO of $C_d - h_{min} - T_{max}$ for TRB 30204.

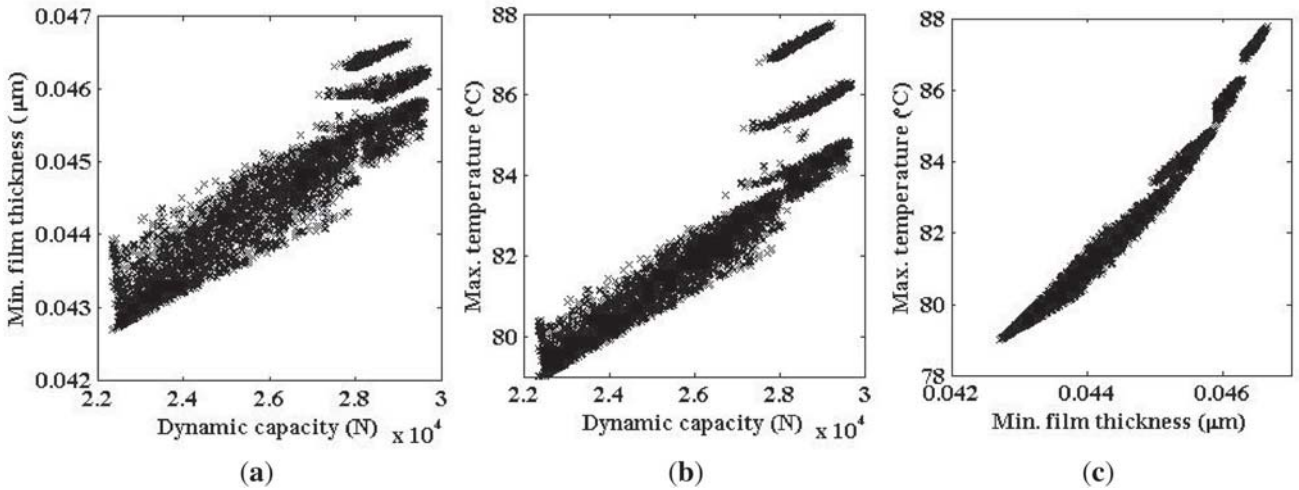

Figure 11. Projection of POS figure 10 onto the (**a**) $C_d - h_{min}$, (**b**) $C_d - T_{max}$ and (**c**) $h_{min} - T_{max}$ planes.

population of 1000 and 100 generations for bearing 6202, we found that it takes 20.37 seconds for single objective optimization. To get a Pareto front of 50 it will take 50 multiply by 20.37, which is 1018.5 seconds. But if we apply NSGA-II to get Pareto optimal solution, it gets there in single run of code which is 19.45 seconds for 1000 population and 100 generations.

EAs performs with the population of results as a replacement of a single result in individual step. In view of previously stated aspects, the evolutionary procedure has been selected for resolving the MOOP of TRBs. Evolutionary procedures accessible for resolving the MOOP are Distance-based Pareto GA (DPGA), Strength Pareto Evolutionary Algorithm (SPEA), Pareto Archived Evolutionary Strategy (PAES) and Elitist Non-dominated Sorting Genetic Algorithm (NSGA-II) [25]. Among them the NSGA-II has been selected for resolving the MOOP of TRBs, as it practices the elite-preserving scheme, the categorical diversity-preserving tool and its global skill to uphold an improved result range [25]. Previous 20 years, numerous investigation has been accomplished on Multi-Objective Evolutionary Algorithms (MOEAs) and in the area of evolutionary calculation, MOEAs are being the widespread investigation and application subjects.

5. NSGA-II application to the design of TRBs

This section deals with the implementation of NSGA-II to the design of TRBs and gives the results thus obtained.

5.1 *NSGA-II computer program*

Optimization of TRB design was performed by using NSGA-II computer program developed by the research centre kanGAL, IIT Kanpur. It is developed in C^{++} language, alterations have been performed in it, to aid in resolving the MOOP of rolling bearings. Depending upon the optimization formulation the associated objective

Table 10. STA of C_d.

	Augmented design variables											Internal geometric parameters obtained using augmented design variables							
Bearing no.	D_m mm	D_r mm	Z	l_e mm	$K_{D_{min}}$	$K_{D_{max}}$	ε	e	β	α_o	ζ	$S^o_{2_{min}}$ mm	$S^i_{1_{min}}$ mm	$B_{1_{min}}$ mm	$B_{2_{min}}$ mm	$C_{1_{min}}$ mm	$C_{2_{min}}$ mm	β°	C_d N
30204	34.3	6.6	16	8.9	0.400	0.600	0.4711	0.070	0.949	15.5	0.250	1.7	2.9	1.1	2.2	1.0	0.5	2.5	29963
30205	38.7	6.7	18	10.0	0.399	0.598	0.4962	0.069	0.948	16.8	0.240	1.7	2.4	1.3	2.0	1.0	0.5	2.5	36077
32205	38.3	5.5	22	12.4	0.369	0.587	0.4976	0.070	0.948	20.9	0.248	1.7	2.1	1.3	2.8	1.0	0.5	2.6	39383
322/28	43.3	5.9	23	13.6	0.357	0.599	0.5000	0.069	0.946	21.4	0.250	1.7	2.6	1.4	2.6	1.0	0.5	2.5	47333
30206	46.4	8.0	18	11.0	0.390	0.599	0.4979	0.062	0.933	16.0	0.250	2.1	3.0	1.5	1.8	1.0	0.5	2.3	47087
32206	45.5	8.8	16	14.1	0.363	0.600	0.4506	0.068	0.934	16.2	0.250	1.7	1.9	1.7	2.5	1.0	0.5	2.6	58427
30306	54.7	9.5	18	11.8	0.384	0.597	0.4332	0.070	0.948	18.0	0.248	1.9	6.3	2.6	2.9	2.0	0.9	2.6	59353
32207	53.5	9.8	17	14.7	0.384	0.599	0.4666	0.070	0.927	16.4	0.250	2.1	2.9	2.9	3.7	2.0	1.0	2.5	70294
32208	59.9	10.9	17	14.7	0.397	0.600	0.4315	0.070	0.948	16.2	0.235	2.4	3.0	2.7	4.0	2.0	1.0	2.5	79238

Table 11. STA of h_{min}.

	Augmented design variables											Internal geometric parameters obtained using augmented design variables							
Bearing no.	D_m mm	D_r mm	Z	l_e mm	$K_{D_{min}}$	$K_{D_{max}}$	ε	e	β	α_o	ζ	$S^o_{2_{min}}$ mm	$S^i_{1_{min}}$ mm	$B_{1_{min}}$ mm	$B_{2_{min}}$ mm	$C_{1_{min}}$ mm	$C_{2_{min}}$ mm	β°	h_{min} μm
30204	35.2	5.7	19	8.9	0.400	0.600	0.500	0.070	0.950	15.6	0.250	1.6	3.8	1.0	2.3	1.0	0.5	2.2	0.04719
30205	39.8	5.6	22	10.0	0.368	0.600	0.494	0.068	0.949	16.8	0.232	1.7	3.4	1.1	2.2	1.0	0.5	2.0	0.05329
32205	38.6	5.3	23	12.0	0.350	0.599	0.484	0.068	0.921	20.9	0.192	1.7	2.4	1.6	2.9	1.4	0.5	2.5	0.05136
322/28	43.4	5.9	23	13.3	0.360	0.599	0.500	0.069	0.940	21.4	0.250	1.7	2.7	1.7	2.6	1.2	0.5	2.5	0.05818
30206	49.1	5.8	26	11.1	0.327	0.595	0.497	0.070	0.939	17.8	0.249	1.7	5.2	1.2	2.1	1.0	0.5	1.9	0.06437
32206	48.0	6.4	23	14.0	0.377	0.599	0.500	0.070	0.949	16.4	0.247	1.6	4.2	1.3	3.0	1.1	0.5	1.9	0.06412
30306	56.4	7.9	22	11.8	0.351	0.591	0.494	0.070	0.945	18.5	0.249	1.8	7.7	2.3	3.2	2.0	0.9	2.3	0.07463
32207	56.1	7.5	23	14.8	0.382	0.600	0.500	0.070	0.950	17.4	0.250	1.8	5.0	2.6	4.1	2.0	1.0	2.0	0.07435
32208	63.4	8.1	24	14.8	0.374	0.600	0.500	0.070	0.944	17.9	0.234	1.8	5.8	2.3	4.3	2.0	1.0	2.0	0.08338

Table 12. STA of T_{max}.

	Augmented design variables											Internal geometric parameters obtained using augmented design variables							
Bearing no.	D_m mm	D_r mm	Z	l_e mm	$K_{D_{min}}$	$K_{D_{max}}$	ε	E	β	α_o	ζ	$S^o_{2_{min}}$ mm	$S^i_{1_{min}}$ mm	$B_{1_{min}}$ mm	$B_{2_{min}}$ mm	$C_{1_{min}}$ mm	$C_{2_{min}}$ mm	β°	T_{max} °C
30204	33.2	6.7	14	6.5	0.300	0.500	0.401	0.010	0.800	11.8	0.125	2.7	2.7	1.7	3.9	1.8	1.8	2.0	79
30205	38.3	6.0	18	4.4	0.301	0.501	0.402	0.011	0.807	13.2	0.135	3.2	3.2	3.4	5.3	3.5	3.3	1.8	80
32205	38.2	5.4	20	4.5	0.308	0.504	0.428	0.027	0.803	20.0	0.133	3.2	3.2	5.3	6.4	5.0	3.9	2.4	82
322/28	42.8	6.1	20	4.9	0.304	0.502	0.405	0.015	0.843	20.2	0.184	3.5	3.6	5.6	6.7	5.1	4.4	2.5	86
30206	45.8	7.2	18	5.0	0.301	0.501	0.402	0.011	0.809	11.8	0.128	3.8	3.8	3.6	5.6	3.6	3.6	1.6	87
32206	45.8	7.2	18	5.6	0.300	0.506	0.406	0.010	0.800	12.4	0.126	3.8	3.8	5.1	7.4	5.1	4.5	1.7	89
30306	50.7	10.5	14	6.6	0.300	0.500	0.400	0.010	0.802	10.0	0.126	4.7	4.7	3.5	6.9	3.7	3.7	1.7	94
32207	53.1	9.4	16	6.8	0.322	0.516	0.405	0.012	0.811	15.3	0.200	3.7	3.7	6.0	8.3	5.2	5.2	2.3	96
32208	59.6	10.6	16	7.2	0.300	0.520	0.402	0.014	0.801	15.3	0.135	3.8	3.8	5.6	8.3	5.0	5.0	2.3	101

Table 13. MTA of C_d and h_{min}.

	Augmented design variables											Internal geometric parameters obtained using augmented design variables								
Bearing no.	D_m mm	D_r mm	Z	l_e mm	$K_{D_{min}}$	$K_{D_{max}}$	ε	e	β	α_o	ζ	$S^o_{2_{min}}$ mm	$S^i_{1_{min}}$ mm	$B_{1_{min}}$ mm	$B_{2_{min}}$ mm	$C_{1_{min}}$ mm	$C_{2_{min}}$ mm	β°	C_d N	h_{min} μm
30204	34.3	6.6	16	8.9	0.386	0.588	0.452	0.067	0.937	15.6	0.235	1.6	2.9	1.2	2.1	1.0	0.5	2.5	29960	0.04634
30205	39.6	5.8	21	10.0	0.373	0.597	0.498	0.067	0.944	16.8	0.243	1.7	3.2	1.1	2.2	1.0	0.5	2.1	34846	0.05327
32205	38.0	5.7	21	12.4	0.356	0.596	0.466	0.069	0.941	20.9	0.244	1.7	1.9	1.3	2.8	1.0	0.5	2.7	39813	0.05134
322/28	42.8	6.5	21	13.5	0.390	0.580	0.495	0.068	0.934	21.4	0.237	1.7	2.2	1.6	2.4	1.0	0.5	2.8	48298	0.05814
30206	46.4	8.0	18	11.0	0.332	0.599	0.484	0.053	0.946	15.9	0.241	2.2	3.0	1.5	1.8	1.0	0.5	2.3	47023	0.06329
32206	45.8	8.3	17	14.1	0.369	0.592	0.470	0.046	0.886	15.6	0.188	1.9	2.3	1.5	2.7	1.0	0.5	2.4	57154	0.06282
30306	54.8	9.5	18	11.8	0.316	0.522	0.418	0.063	0.885	18.3	0.237	1.9	6.3	2.6	2.9	2.0	0.9	2.7	59400	0.07379
32207	53.3	9.6	17	14.6	0.373	0.597	0.423	0.066	0.922	15.6	0.246	2.4	2.9	2.8	3.9	2.0	1.0	2.4	69330	0.07225
32208	60.0	10.9	17	14.7	0.369	0.599	0.426	0.068	0.936	16.5	0.236	2.3	3.1	2.7	3.9	2.0	1.0	2.5	79064	0.08140

Table 14. MTA of C_d and T_{max}.

	Augmented design variables											Internal geometric parameters obtained using augmented design variables								
Bearing no.	D_m mm	D_r mm	Z	l_e mm	$K_{D_{min}}$	$K_{D_{max}}$	ε	E	β	α_o	ζ	$S^o_{2_{min}}$ mm	$S^i_{1_{min}}$ mm	$B_{1_{min}}$ mm	$B_{2_{min}}$ mm	$C_{1_{min}}$ mm	$C_{2_{min}}$ mm	β°	C_d N	T_{max} °C
30204	33.8	6.9	15	8.8	0.327	0.583	0.430	0.064	0.922	14.5	0.196	1.9	2.6	1.1	2.2	1.0	0.5	2.5	29786	84
30205	38.0	7.4	15	9.7	0.327	0.540	0.446	0.036	0.846	16.5	0.152	1.8	1.8	1.6	1.9	1.2	0.5	2.7	34303	87
32205	37.9	6.3	19	11.0	0.333	0.599	0.499	0.066	0.900	20.9	0.190	1.7	1.7	2.7	2.7	2.2	0.6	2.9	37314	93
322/28	42.3	7.1	19	12.8	0.338	0.551	0.429	0.035	0.888	21.2	0.195	1.8	1.8	2.3	2.4	1.5	0.6	3.0	47513	100
30206	46.4	8.0	18	10.9	0.364	0.598	0.494	0.055	0.895	15.9	0.245	2.2	3.1	1.5	1.8	1.0	0.6	2.3	46691	99
32206	45.4	8.8	16	13.9	0.301	0.591	0.439	0.048	0.937	15.9	0.196	1.8	1.9	1.7	2.7	1.1	0.6	2.6	57542	101
30306	52.4	10.8	15	11.6	0.381	0.590	0.419	0.058	0.889	15.2	0.241	2.8	4.7	2.5	3.1	2.0	0.9	2.6	59254	106
32207	52.9	10.3	16	14.5	0.344	0.536	0.424	0.047	0.883	16.3	0.173	2.2	2.4	3.0	3.7	2.0	1.1	2.6	70346	109
32208	59.3	11.5	16	14.6	0.332	0.595	0.400	0.032	0.839	16.3	0.202	2.3	3.1	2.7	3.9	2.0	1.0	2.5	79731	113

Table 15. MTA of h_{min} and T_{max}.

	Augmented design variables											Internal geometric parameters obtained using augmented design variables								
Bearing no.	D_m mm	D_r mm	Z	$l_e$mm	$K_{D_{min}}$	$K_{D_{max}}$	ε	e	β	α_o	ζ	$S^o_{2_{min}}$ mm	$S^i_{1_{min}}$ mm	$B_{1_{min}}$ mm	$B_{2_{min}}$ mm	$C_{1_{min}}$ mm	$C_{2_{min}}$ mm	β°	h_{min} μm	T_{max} °C
30204	33.2	6.9	14	6.5	0.303	0.517	0.410	0.022	0.842	12.2	0.131	2.6	2.6	2.0	3.5	2.1	1.5	2.1	0.04278	79
30205	38.2	7.2	15	9.6	0.338	0.544	0.451	0.039	0.913	16.8	0.217	1.7	1.9	1.6	1.9	1.3	0.6	2.65	0.05147	87
32205	38.2	6.0	19	11.0	0.331	0.527	0.443	0.030	0.917	20.8	0.125	1.7	2.0	2.7	2.7	2.3	0.5	2.78	0.05070	94
322/28	42.6	6.9	18	11.4	0.341	0.598	0.494	0.044	0.811	21.4	0.193	2.0	2.2	3.0	3.0	2.3	1.2	2.94	0.05637	97
30206	46.9	7.9	18	10.3	0.347	0.580	0.473	0.059	0.926	17.8	0.229	1.8	3.2	1.9	2.1	1.2	1.1	2.56	0.06324	99
32206	45.7	8.9	15	13.2	0.323	0.589	0.426	0.031	0.855	16.4	0.247	1.7	2.1	2.6	2.6	1.9	0.6	2.65	0.06185	99
30306	54.7	9.6	17	10.4	0.318	0.581	0.400	0.049	0.813	18.5	0.243	2.0	6.3	3.4	3.5	2.7	1.5	2.73	0.07217	110
32207	53.3	10.2	15	13.7	0.365	0.597	0.420	0.034	0.943	16.6	0.243	2.2	2.6	3.8	3.8	2.8	1.2	2.65	0.07114	107
32208	59.9	11.2	16	14.0	0.353	0.562	0.400	0.027	0.862	16.4	0.186	2.3	3.0	3.4	3.9	2.7	1.0	2.56	0.08049	113

Table 16. MTA of C_d, h_{min} and T_{max}.

Bearing no.	Augmented design variables											Internal geometric parameters obtained using augmented design variables								
	D_m mm	D_r mm	Z	l_e mm	$K_{D_{min}}$	$K_{D_{max}}$	ε	e	β	α_o	ζ	$S^o_{2_{min}}$ mm	$S^i_{1_{min}}$ mm	$B_{1_{min}}$ mm	$B_{2_{min}}$ mm	$C_{1_{min}}$ mm	$C_{2_{min}}$ mm	β°	C_d N	h_{min} µm	T_{max} °C
30204	34.3	6.6	16	8.8	0.380	0.586	0.463	0.056	0.883	15.4	0.189	1.7	2.9	1.2	2.2	1.1	0.5	2.5	29638	0.04623	86
30205	38.1	7.3	15	9.5	0.355	0.597	0.443	0.055	0.914	16.6	0.152	1.7	1.9	1.8	1.9	1.4	0.6	2.7	33433	0.05135	86
32205	38.3	5.5	22	11.9	0.302	0.595	0.498	0.016	0.909	20.8	0.143	1.8	2.2	1.6	3.0	1.4	0.6	2.5	38052	0.05118	99
322/28	42.6	6.7	20	13.2	0.317	0.598	0.438	0.050	0.867	21.4	0.231	1.7	2.1	2.0	2.4	1.3	0.5	2.9	47920	0.05794	102
30206	46.4	8.0	18	10.9	0.363	0.573	0.478	0.065	0.894	16.0	0.249	2.1	3.1	1.5	1.8	1.0	0.5	2.3	46878	0.06327	99
32206	46.0	8.4	17	13.7	0.343	0.597	0.445	0.041	0.879	16.4	0.240	1.7	2.4	1.9	2.7	1.3	0.6	2.5	56631	0.06303	103
30306	52.6	10.8	15	11.3	0.328	0.571	0.413	0.061	0.873	15.6	0.248	2.6	4.8	2.8	3.1	2.2	0.9	2.6	58268	0.07067	106
32207	53.1	10.2	16	14.5	0.345	0.537	0.435	0.041	0.872	16.3	0.228	2.2	2.5	3.1	3.7	2.1	1.0	2.6	69602	0.07200	109
32208	59.4	11.5	16	14.2	0.313	0.580	0.402	0.028	0.845	16.0	0.188	2.5	2.6	3.1	4.0	2.3	1.0	2.6	78108	0.08034	112

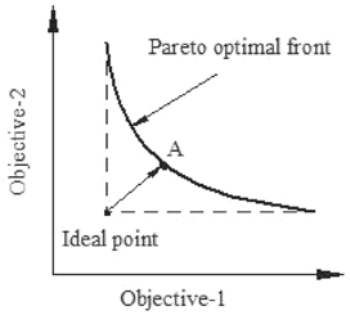

Figure 12. The ideal point and the corresponding knee point 'A' in a Pareto front.

objectives, constraints, design parameter limits, periphery sizes of bearings and values of GA variables could be inserted in the unit to acquire optimized bearing outcomes. In this unit design variables can be signified as binary-coded chromosomes or real-coded chromosomes.

In the current formulation, three objectives, twenty-eight constraints and eleven design variables are combined in the NSGA-II computer program. Design variables defined in real-coded chromosomes and suitable alterations have been completed in NSGA-II computer program to take number of rollers as an integer. A block diagram of the NSGA-II procedure is presented in figure 6. For basic terminologies and concepts of the GA refer to [25].

5.2 *Design variable bounds*

Material properties and other constants, the lubricant data of grease at 100°C and air properties at 40°C are provided in tables 4, 5 and 6, respectively. Design variables are assigned the bound, to diminish the result space and are found by using standard TRB dimensions (refer table 7). Constraints 1-8 are used to find out the bounds of D_m, D_r, Z and l_e. Bounds of α_o are taken from [18]. Remaining constraint factors' bounds are taken from [8]. All eleven design variable bounds are provided in table 8.

5.3 *Tuning of GA parameters and convergence study*

Computations were executed on i5-4200M CPU @ 2.50GHz Intel processor with 4GB RAM using Dev C^{++}. The population reserved as 5000 for all cases. In the present problem, we are taking a large value of population because it was found that very few solutions qualified constraint violation, so to get enough solutions on the Pareto front a large population is required. For lower size of population narrow and/or scattered Pareto front was found. On fixing the population number, GA variables (i.e., the crossover probability, the mutation probability, the crossover index, the mutation index and the random seed) were changed to

Table 17. Matching of dynamic load rating and their corresponding life assessment factors.

		By the augmentation of									
		C_d		C_d -h_{min}		C_d -T_{max}		C_d -h_{min} -T_{max}		C_d Ref. [13]	
Bearing no.	C_{d_std} (N)	C_d (N)	λ_l	C_d (N)	λ_l	C_d (N)	λ_l	C_d (N)	λ_l	C_d (N)	λ_l
30204	27500	29962.62	1.33	29960.38	1.33	29785.60	1.30	29637.75	1.28	31220	1.53
30205	30800	36077.41	1.69	34845.84	1.51	34302.79	1.43	33433.33	1.31	34810	1.50
32205	35800	39383.46	1.37	39813.06	1.42	37314.49	1.15	38051.68	1.23	40600	1.52
322/28	41800	47332.77	1.51	48297.9	1.62	47513.24	1.53	47919.39	1.58	48540	1.64
30206	40200	47086.73	1.69	47022.7	1.69	46690.97	1.65	46878.06	1.67	–	–
32206	50100	58426.63	1.67	57153.86	1.55	57542.28	1.59	56630.77	1.50	52250	1.15
30306	56100	59353.21	1.21	59400.21	1.21	59253.93	1.20	58267.77	1.13	59350	1.21
32207	66000	70294.29	1.23	69329.59	1.18	70346.23	1.24	69601.84	1.19	69810	1.20
32208	74800	79237.82	1.21	79064.16	1.20	79731.20	1.24	78108.25	1.16	75420	1.03

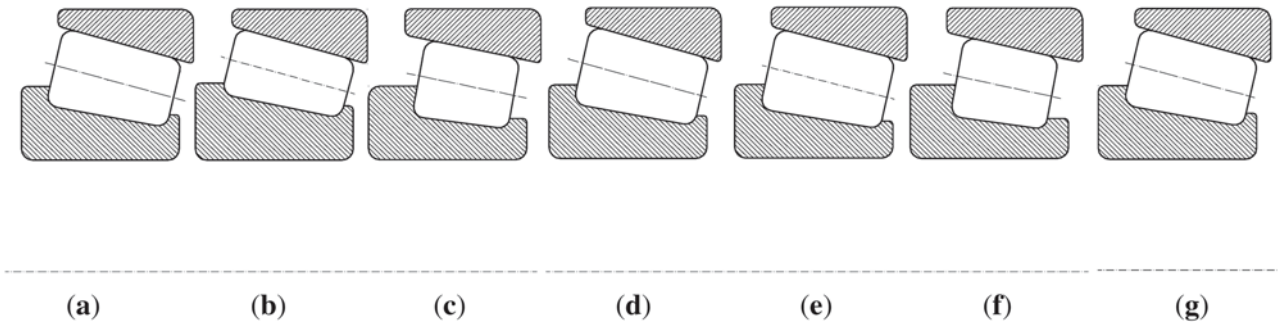

Figure 13. Radial dimensions of TRBs by the augmentation of (a) C_d, (b) h_{min}, (c) T_{max}, (d) C_d- h_{min}, (e) C_d- T_{max}, (f) h_{min}- T_{max} and (g) C_d- h_{min}-T_{max}

acquire the maximization of results (i.e., the varied and capitalized solutions, when objectives are of the maximizing kind). The crossover probability is changed as 0.7-0.9 and the value of mutation probability changed as 0.1-0.2. Crossover distribution and mutation distribution indices are presented from the usage of real-coded chromosomes. These were allocated quantities so as to attain the maximum diverse of result values. Mostly, lesser values of these distribution indices provide varied results and thus improved estimate of the POF/POS. To produce preliminary population for each run the random seed was utilized. It was changed as 0-1. The values of GA parameters were chosen such that it would give maximum value to the objective function in the maximization problem. Variation of GA factors and preferred numbers are presented in table 9. Originally, the procedure was prepared to execute with some number of generations and then generations are optimized in sequence until the convergence has reached. For TRB 30204, figure 7 through figure 9 show the dual-objective optimization of $C_d - h_{min}$, $C_d - T_{max}$ and $h_{min} - T_{max}$; In figure 7, POFs are shown for the 20, 30, 50 and 80 generations, which depict the gradual converge of final solutions. In final generation, the POF has discrete solution location due to the number of roller to be taken as an integer design parameter. In figure 8, POFs are shown for the 10, 20 and 50 generations, herein the convergence has reached much earlier at 50 generations. The discrete POFs can be seen due to discrete number of roller is to be chosen. Figure 9 shows similar observation but herein convergence has taken place at 30 generations itself. Figure 10 shows the converged triple-objective optimized POS at 40th generations. Discrete nature of POSs could be seen and all three objectives looks to be independent due to wide spread nature of POSs in figure 10. Figures 11 (a), (b) and (c) are the projections of POS (figure 10) on to different two-dimensional planes, which shows POF by keeping one of objective value constant. Herein also, the trends corroborate with previous characteristics of POFs.

5.4 *Numerical Illustrations*

Optimised solutions of the single objective optimization of C_d,h_{min} and T_{max} are presented in table 10, 11, 12. Whereas, table 13, 14, 15 display the dual-objective optimized solutions and table 16 presents triple-objective optimized solutions for several sizes of bearings that are deliberated. In bearing catalogues we get the information of dynamic

Table 18. Tolerances for variables and targets from susceptivity analysis.

Perturbed variables			Feasible tolerances											
			D_m (μm)		D_r (μm)		l_e (μm)		C_d (N)		h_{min} (pm)		T_{max} (°C)	
D_m	D_r	l_e	Min.	Max.	Min.	Max.	Min.	Max	Min.	Max.	Min.	Max.	Min.	Max.
↘	↗	↗	-33.463	+18.897	–	–	–	–	−01.491	+00.837	−44	+25	−0.05075	+0.02877
↗	↘	↗	–	–	−33.027	+09.567	–	–	−158.74	+46.00	−39	−14	−0.0132	+0.00379
↗	↗	↘	–	–	–	–	−43.783	+43.863	−115.36	+115.45	−30	+30	−0.06985	+0.06995
↘	↘	↗	−20.623	+48.457	−32.166	+10.791	–	–	−153.80	+52.14	−38	+27	−0.03105	+0.0613
↘	↗	↘	−42.563	+26.287	–	–	−43.089	+43.716	−113.76	+114.41	−80	+39	−0.124	+0.0775
↗	↘	↘	–	–	−33.003	+09.971	−43.512	+43.716	−259.61	+154.29	−65	+39	−0.07953	+0.07286
↘	↘	↘	−36.023	+45.347	−32.443	+10.791	−43.483	+41.629	−265.94	+89.86	−83	+32	−0.11924	+0.08119

capacities only, which we have compared in terms of life factors in table 10. Since bearing catalogues do not give internal design of bearings so elastohydrodynamic minimum film thickness and maximum temperature cannot be obtained. Hence, without the information of elastohydrodynamic minimum film thickness and maximum temperature values we cannot represent a design point on the Pareto front. Among results on the POF/POS, merely single result named as the knee result or knee, is depicted in tables 13, 14, 15 and 16, for each TRB. The knee result is the outcome in the trade-off front such that it is at a least distance from the ideal point (see figure 12). In fact, any point on the POF/POS is an optimal point, but for uniformity in the analysis the knee point has been chosen. Physically, knee point is the point in Pareto front where drastic change in objective functions are observed at neighbouring points in the front.

We have also plotted Pareto optimal surface by optimizing all the three objectives together. Figure 11 is the projection of Pareto optimal surface generated when all the three objectives have been optimized simultaneously. Knee points have been calculated for Pareto fronts with two objectives at a time, which has been represented in tables 13, 14 and 15.

POFs gives a range of non-dominated solution, which allows designer to choose a solution after optimisation has been done. It is superior to classical techniques, where the designer needs to give several combinations of weights to objective function before optimisation and the whole process of optimisation is carried out several times for getting different solutions. To match the life of optimized TRBs with standard bearings a *life assessment factor* (λ_l) is utilized. It is pointed that Eq.(19) is attained from Eq. (8). Let C_{d_new} and C_{d_std} are the dynamic load rating of the optimized and standard bearings, respectively. Hence,

$$\lambda_l = (C_{d\_new}/C_{d\_std})^{10/3} \tag{19}$$

Dynamic capacities of optimized bearings and life assessment factors are compared with standard catalogue values and with ref. [13], which is shown in table 17. Average running time of the algorithm (for each bearing) for the SOO was 307 s, for the DOO it was 230 s and for the TOO it was 220 s. Figure 13 matches radial dimensions of the optimized bearing acquired by the SOO, the DOO and the TOO of TRB 30204. For instance, the optimization with thermal considerations gives TRBs with lesser roller length. This can be interpreted as, the decrease in the roller length decreases the heat transfer due to the reduction in surface area of the roller.

6. Sensitivity analysis

During production of different bearing components, due to diverse causes (i.e., the man, machine and material) it is challenging to achieve precise design variable values and

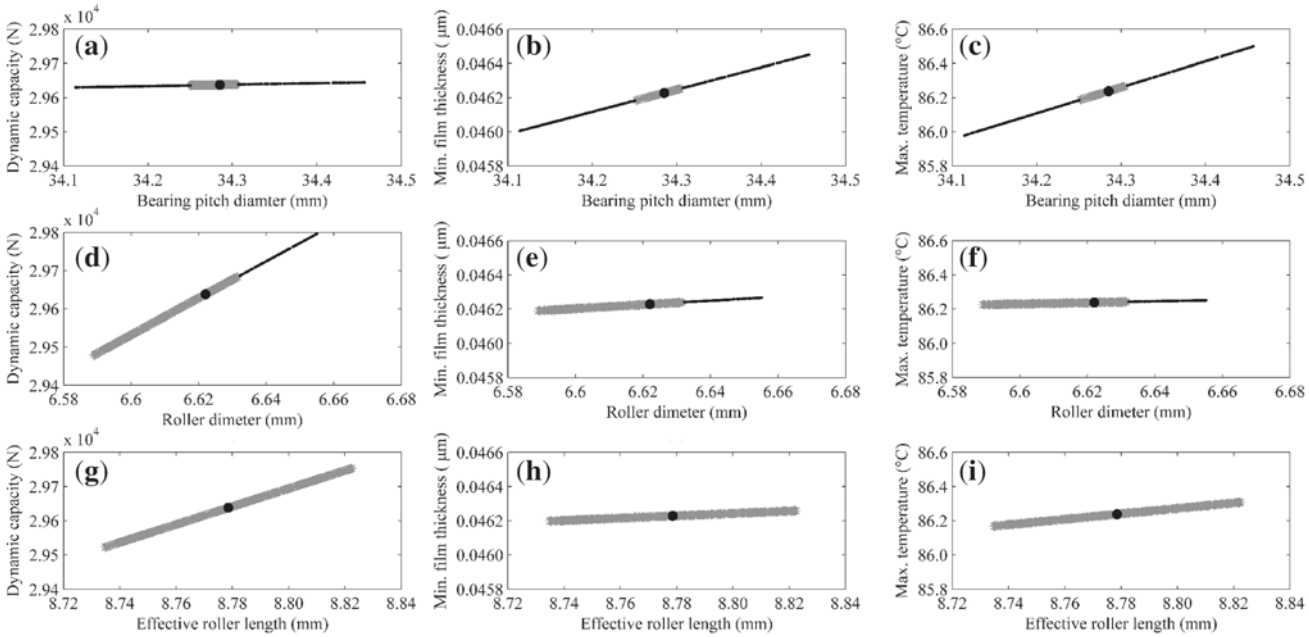

Figure 14. Susceptivity analysis plots of three design parameters D_m, D_r and l_e with the targets (black solid line, Infeasible results, gray solid line, Feasible results, filled circle, TTA result).

up to 1.0% deviation may take place in these. Precision can be found from standard bearing catalogue depending upon bearing class chosen. The American Bearing Manufacturers Association (ABMA) has defined several classes for tolerance for the roller and ball bearing. The ABMA's RBEC (roller bearing engineers' committee) Class 1 or ISO (International organization for Standardization) normal class tolerances have been referred, which is the most basic class allowing maximum tolerances. For engineers the sensitivity investigation permits to evaluate the causes and origins of uncertainties, in the interest of constructing vigorous design. This section tries to assess the sensitivity of objectives with design variables. Among eleven design variables, variables D_m, D_r and l_e are considered for the sensitivity investigation since they directly regulate the objective function and are susceptible to industrial tolerances. For present analysis, we will diverge these design variables by an extreme of $\pm 1\%$ about a knee point, exclusively and concurrently, and attempt to investigate the sensitivity of three objective expression values.

For the illustration, the sensitivity study is done on TRB model 30204. For the bearing, the individual design parameters (D_m, D_r and l_e) were disturbed independently (with entire remaining design variables fixed) and by means of groupings of entire three design variables in a disturbance range of $\pm 1\%$ around the knee point result. As a consequence, an overall populations of 500 disturbed points were acquired and resultant objective expression was assessed in individual case. Among them merely limited populations become feasible solutions. The maximum and minimum values (tolerances) of disturbed design variables and objective expression values in the populations of viable results are displayed in table 18. It is to be kept in mind that the maximum / minimum value of design variables in the table do not inevitably represent to the maximum / minimum of the objective expression. The deviation of C_d, h_{min} and T_{max} with the disturbance of three parameters are depicted in figure 14.

7. Observations and discussions

This section is going to interpret numerical illustrations that are presented in the previous section.

- A very narrow range of the convergence of constraint constants has been observed.
- POFs and the POS obtained by the DOO and the TOO showed that objectives taken for optimization are conflicting, i.e., objectives are compromising with each other. The advantage of the POF/POS is that the designer can choose any solution on the POF/POS according to the requirement.
- Discontinuity has been observed in POFs and the POS and it is due to the reason that Z takes an integer value only. Thus a continuous variation of this design variable is not possible.
- The SOO life comparison factors have been found to vary from 1.21 to 1.69.
- The DOO of C_d -h_{min} and C_d -T_{max} has given the life comparison factors of 1.18-1.69 and 1.15-1.65, respectively; whereas TOO values ranges from 1.13-1.67.

- The most of the DOO and TOO objective values are less than that of SOO values, but few MOO values are more than SOO values. This betterment of MOO values than SOO values is due to the reason that SOO values may lockup at the local optima but the MOO space provides more freedom to explore since it uses inherent diversity by the principle of dominance that leads to better convergence and less chance to get stuck at local minima.
- In the present work more number of constraints have been taken into consideration to make the design feasible. Constraint number 27 and 28 are the extra constraints that has been introduced in this work that are affecting the small bearings. So it can be observed that three initial bearings of the series have less value of C_d.
- The sensitivity analysis plot (i.e. figure 14) shows that the viable region for D_m is lesser than for D_r. Hence, during designing tighter tolerances should be retained for D_m than D_r; Within $\pm 1\%$tolerance zone, l_e having all feasible solutions; Maximum temperature is having very less significant variation with three variables.

8. Conclusions

The present work demonstrated the multi-objective optimization of standard TRBs design, by taking into account the dynamic load rating, the elasto-hydrodynamic minimum film thickness and the maximum bearing temperature as objectives. The NSGA-II has been used as an optimization tool for this design. Three objectives C_d, h_{min} and T_{max} turned out to be conflicting and corresponding POFs and the POS have obtained. The benefit of POF/POS is that designer can choose any solution on the POF/POS according to the requirement. It is illustrated that the multi-objective optimization space provides more freedom to explore since it uses inherent diversity by the principle of dominance that leads to better convergence as compared to single objective optimization and less chance to get stuck at local minima. Optimized bearings showed the enhanced lives than standard TRBs, this demonstrates the significance of optimization to engineering design formulations and essential to advance prevailing design of TRBs. Besides optimizing standard TRBs, this design methodology could be used to design non-standard TRBs also. To evaluate the sensitivity of three objectives with design variables, a sensitivity analysis has been performed on the TOO knee point solution. From the sensitivity analysis data, tolerances of three design variables and three objective expressions have been provided. Tolerances on design variables, thus provided, could be utilised during production of TRBs, to evade any substantial deviation in objective expressions. In a nut shell, this methodology of optimizing and sensitivity analyses of TRBs could be implemented during designing and manufacturing of standard TRBs. It would be interesting to perform experiments on optimized bearings to check the increment of life of bearings. Apart from this using the finite element method and data mining techniques as an alternative method the dynamic load rating in tapered roller bearings could be determined for the verification of optimized TRBs.

Nomenclatures

A	Area normal to the heat flow, m^2
A_f	Area of the flange, mm^2
b_m	Rating factor for the contemporary material
B	Width of the cone, mm
$B_{1_{\min}}$	Width of the narrow front face of cone, mm
$B_{2_{\min}}$	Width of the flange, mm
C	Width of the cup, mm
C_d	Dynamic load capacity of the bearing, N
C_{d_new}	Dynamic load capacity of the bearing obtained using NSGA-II, N
C_{d_std}	Dynamic load capacity of the bearing given in bearing catalogues, N
C_p	Specific heat of a lubricant at a conSOOnt pressure, J/Kg-K
$C_{1_{\min}}$	Minimum width of the back-face of the cup, mm
$C_{2_{\min}}$	Minimum width of the front-face of the cup, mm
d	Inner (or bore) diameter of the bearing, mm
d_i	inner raceway mean diameter, mm
d_o	outer raceway mean diameter, mm
D	Outer diameter of the bearing, mm
D_m	Bearing pitch diameter, mm
D_r	Roller mean diameter, mm
$D_{r_{LL}}$	Lower limit of the roller mean diameter, mm
$D_{r_{UL}}$	Upper limit of the roller mean diameter, mm
D_{o_i}	Minimum diameter of the cup, mm
e	Parameter for the mobility condition
E	Modulus of elasticity, Pa
E'	Equivalent modulus of elasticity, Pa
EI	Section modulus of the flange section subjected to bending, $N\text{-}mm^2$
$f(X)$	Objective vector
Gr	Grashof number
h_f	Position of the rib-roller contact on the flange face, mm
h_{min}	Elasto-hydrodynamic minimum film thickness, m
h_r	Radiation heat transfer coefficient
H_w	Housing width, mm
i	Number of rows of the roller
k	Thermal conductivity of rings and the rolling element
$K_{D\min}$	Minimum roller diameter limiter
$K_{D\max}$	Maximum roller diameter limiter
k_o	Thermal conductivity of the lubricant, W/m°C
l	Total length of the roller, mm
l_e	Effective length of the roller, mm

ℓ	DiSOOnce between two points (i, j) of the heat transfer, m
L_{10}	Rating life (Bearing fatigue life cycles)
n_o	Outer raceway speed, rpm
P	Equivalent radial load, N
P_r	Prandtl number of the lubrication oil
Q_i	Load on the inner ring at the most heavily loaded roller, N
Q_{max}	Contact force on the interior raceway at the heaviest loaded roller, N
Q_o	Load on the outer ring at the most heavily loaded roller, N
Q_f	Load on the flange at the most heavily loaded roller, N
r	Corner radius of the roller, mm
r_1	Cone back-face chamfer height, mm
r_2	Cone back-face chamfer width, mm
r_3	Cup back-face chamfer height, mm
r_4	Cup back-face chamfer width, mm
r_5	Chamfer height and width of the front-face the cone and the cup, mm
Re	Reynolds number
$R_{e_{i,o}}$	Equivalent radius (m)
$S^i_{1_{min}}$	Minimum thickness of the front-face of the cone, mm
$S^i_{2_{min}}$	Minimum thickness of the back face of the cone, mm
$S^o_{1_{min}}$	Minimum thickness of the back-face of the cup, mm
$S^o_{2_{min}}$	Minimum thickness of the front-face of the cup, mm
th	Seal thickness, mm
T	Total width of the bearing, mm
T_i and T_j	Temperatures of the two points (i, j) between which the heat transfer is taking place
T_l	Lubricant temperature, °C
T_{max}	Maximum bearing temperature, °C
$u_{i,o}$	Entrainment velocity, m/s
u_s	1/3rd of the surface velocity of the housing, m/s
X	Design variable vector
Z	Number of rollers

Greek letters

α_f	Flange angle
α_i	Contact angle of the inner raceway (i.e., cone)
α_o	Outer raceway contact angle
α_p	Pressure viscosity coefficient of lubricant, m^2/N
β	Parameter for the effective length of the roller
β^o	Semi taper angle of the roller
γ	Ratio, $D_{r_{mean}} \cos \alpha_o / D_m$
ε	Parameter for outer ring strength consideration
ε_h	Thermal emissivity of the housing
η_o	Dynamic viscosity of lubricant, N-s/m^2
λ	Reduction factor to account for the edge loading and the non-uniform stress
λ_l	Life comparison factor
ν	Factor to account for the edge loading
ν_o	Kinematic viscosity of lubricant, m^2/s
σ_{b_f}	Bending stress in the flange, N/mm^2
$\sigma_{f_{max}}$	Maximum stress in the flange, N/mm^2
σ^l_{max}	Maximum contact stress, N/mm^2
σ_{safe}	Safe contact stress, N/mm^2
σ_{tf}	Direct tensile stress in the flange, N/mm^2
τ_f	Shear stress in the flange, N/mm^2
υ	Poisson's ratio
ω_m	Angular velocity of the cage, rad/s
ω_r	Angular velocity of the roller, rad/s
ω_o	Angular velocity of the outer raceway, rad/s
ϖ	Width of the structure, m

Subscripts and superscripts

f	Flange
i	Represents the inner raceway or cone
o	Represents the outer raceway or cup

Abbreviations and acronyms

DOO	Dual Objective Optimization
MOO	Multi Objective Optimization
POF	Pareto Optimal Front
POS	Pareto Optimal Surface
SOO	Single Objective Optimization
TOO	Triple Objective Optimization
TRB	Tapered Roller Bearing

Appendix A: Geometrical Parameters and Their Relationships for TRBs

Following equations are used in the present study on the MOO of TRBs [13]

The minimum thickness of the front face of the cup, (refer figure 2)

$$S^o_{2_{min}} = \frac{1}{2}D - \left\{\frac{1}{2}D_m \text{cosec}(\alpha_o - \beta^o) + \frac{1}{2}l\right\} \sec\beta^o \sin\alpha_o \tag{A.1}$$

The minimum thickness of the front face of the cone, (refer figure 2)

$$S^i_{1_{min}} = \left\{\frac{1}{2}D_m \text{cosec}(\alpha_o - \beta^o) - \frac{1}{2}l\right\} \sec\beta^o \sin(\alpha_o - 2\beta^o) - \frac{1}{2}d \tag{A.2}$$

The minimum width of the front face of the cup, (refer figure 2)

$$C_{2_{min}} = \left[C + \frac{1}{2}D_{o_i}\cot\alpha_o\right] - \left[\left\{\frac{1}{2}D_m\text{cosec}(\alpha_o - \beta^o) + \frac{1}{2}l\right\}\sec\beta^o\cos\alpha_o\right] \tag{A.3}$$

The minimum thickness of the back face of the cup, (refer figure 2)

$$C_{1_{min}} = C - C_{2_{min}} - \frac{l\cos\alpha_o}{\cos\beta^o} \tag{A.4}$$

The minimum width of the back face of the cup, (refer figure 2)

$$B_{2_{min}} = \left[T + \frac{1}{2}D_{o_i}\cot\alpha_o\right] - \left[\left\{\frac{1}{2}D_m\text{cosec}(\alpha_o - \beta^o) + \frac{1}{2}l\right\}\sec\beta^o\cos(\alpha_o - 2\beta^o)\right] \tag{A.5}$$

The minimum width of the front face of the cone, (refer figure 2)

$$B_{1_{min}} = B - B_{2_{min}} - \frac{l}{\cos\beta^o}\cos(\alpha_o - 2\beta^o) \tag{A.6}$$

The minimum thickness of the back face of the cup, (refer figure 2)

$$S^o_{1_{min}} = \frac{1}{2}D - \left\{\frac{1}{2}D_m - \frac{1}{2}l\sin(\alpha_o - \beta^o)\right\} + \left\{\left(\frac{1}{2}D_r - \frac{1}{2}l\sin\beta^o\right)\cos(\alpha_o - \beta^o)\right\} \tag{A.7}$$

The minimum thickness of the back face of the cone, (refer figure 2)

$$S^i_{2_{min}} = \left\{\frac{1}{2}D_m - \frac{D_r}{2}\cos(\alpha_o - \beta^o) + \frac{l}{2}\sin\beta^o\right\} - \frac{d}{2} \tag{A.8}$$

Force on the spherical face of the roller

$$Q_f = Q_i\cos\alpha_i\frac{(\sin\alpha_o - \tan\alpha_i\cos\alpha_o)}{\sin(\alpha_o + \alpha_f)} \tag{A.9}$$

Normal force on the cup

$$Q_o = Q_i\cos\alpha_i\frac{(\sin\alpha_f + \tan\alpha_i\cos\alpha_f)}{\sin(\alpha_o + \alpha_f)} \tag{A.10}$$

Tensile stress in the flange

$$\sigma_{t_f} = \frac{Q_f\sin\alpha_f}{A_f} \tag{A.11}$$

Area of the flange

$$A_f = \frac{\pi\left(\frac{1}{2}d + S^i_{2_{min}}\right)B_{2_{min}}}{Z} \tag{A.12}$$

Maximum shear stress in the flange

$$\tau_f = 1.5\frac{Q_f\cos\alpha_f}{A_f} \tag{A.13}$$

Bending stress in the flange

$$\sigma_{b_f} = \frac{Q_f h_f\cos^2\alpha_f}{EI} \tag{A.14}$$

Position of the rib-roller contact on the flange face

$$h_f = \frac{\frac{1}{2}d_1 - \left(\frac{1}{2}d + S^i_{2_{min}}\right)}{2\cos\alpha_f} \tag{A.15}$$

Maximum principal stress in the flange

$$\sigma_{f_{\max}} = \frac{\sigma_{t_f} + \sigma_{b_f}}{2} + \sqrt{\left(\frac{\sigma_{t_f} + \sigma_{b_f}}{2}\right)^2 + \tau_f^2} \tag{A.16}$$

References

[1] Andreason S 1973 Load distribution in a tapered roller bearing arrangement considering misalignment. ASME J. Tribol. 2: 84–92

[2] Karna C L 1974 Performance characteristics at the rib roller end contact in tapered roller bearings. ASLE Trans. 17(1): 14–21

[3] Liu J Y 1976 Analysis of tapered roller bearings considering high speed and combined loading. Trans. ASME Lubr. Symp. 98(4): 564–572

[4] Bercea I, Cretu S and Nélias D 2003 Analysis of double-row tapered roller bearings, part-I. Tribol. Trans. 46: 228–239

[5] Blake J J and Truman, C E 2004 Measurement of running torque of tapered roller bearings. Proc. Inst. Mech. Eng. Part J J. Eng. Tribol. 218(4): 239–250

[6] Chakraborty I, KumarV, Nair SB and Tiwari R 2003 Rolling element bearing design through genetic algorithm. Eng. Optim. 35(6): 649–659

[7] Gupta S, Tiwari R and Nair SB 2007 Multi-objective design optimization of rolling bearings using genetic algorithms. Mech. Mach. Theory. 42: 1418–1443

[8] Rao R B and Tiwari R 2007 Optimum design of rolling element bearings using genetic algorithms. Mech. Mach. Theory 42: 233–250

[9] Kumar S K, Tiwari R and Reddy R S 2008 Development of an optimum design methodology of cylindrical roller bearing using genetic algorithms. Int. J. Comput. Methods Eng. Sci. Mech. 9(6): 321–341

[10] Kumar S K, Tiwari R and Prasad P V V N 2009 An optimum design of crowned cylindrical roller bearings using genetic algorithms. Trans. ASME J. Mech. Des. 131(5): 051011 (14 pages)

[11] Lin W Y 2010 Optimum design of rolling element bearings using a genetic algorithm–differential evolution (GA–DE) hybrid algorithm. Proc. Inst. Mech. Eng. Part C J. Mech. Eng. Sci. 225: 1–8

[12] Wang Z, Meng L and Hao W 2011 Optimal design of parameters for four column tapered roller bearing. Appl. Mech. Mater. 63–64: 201–204
[13] Tiwari R, Sunil K K and Prasad P V V N. 2012 An optimum design methodology of tapered roller bearings using genetic algorithms. Int. J. Comput. Methods Eng. Sci. Mech. 13(2): 108–127
[14] Waghole V and Tiwari R 2013 Optimization of needle roller bearing design using novel hybrid methods. Mech. Mach. Theory. 72: 71–85
[15] Tiwari R and Rahul C 2013 Thermal based optimum design of tapered roller bearing through evolutionary algorithm. In: ASME 2013 Gar Turbine, NAL Bangalore, India. Paper no. GT India 2013-3792
[16] Tiwari R and Chandran R M P 2015 Multitude of objectives based optimum designs of cylindrical roller bearings using evolutionary algorithms. ASME J. Tribol. 137(4): 041504-041504-12
[17] Najjari M and Guilbault R 2015 Formula derived from particle swarm optimization (PSO) for optimum design of cylindrical roller profile under EHL regime. Mech. Mach. Theory 90: 162–174
[18] Tiwari R and Chandran R M P 2017 Optimal design of deep-groove ball bearings based on multitude of objectives using evolutionary algorithms. Multidiscip. Model. Mater. Struct. 14(3): 567–588. https://doi.org/10.1108/MMMS-06-2017-0058
[19] Changsen W 1991 Analysis of Rolling Element Bearings. Mechanical Engineering Publications Ltd., London
[20] IS 7461 (part-1) :1993 Bureau of Indian Standards. General plan of boundary dimensions for tapered roller bearings
[21] Harris T A 2001 Rolling Bearing Analysis. John Wiley, New York
[22] Harris T A and Barnsby R M 1998 Tribology performance prediction of aircraft gas turbine main shaft ball bearings. Tribol. Trans. 41(1): 60–68
[23] Jamison W E, Kauzlarich J J and Mochel E V 1975 Geometric effects on rib-roller contact in tapered roller bearing. ASLE Trans. 20: 79–88
[24] Cohon J L 1985 Multicriteria programming: brief review and applications. In: J. S. Gero (Ed.), Design optimization, pp. 163–191. Academic Press, New York
[25] Deb K 2013 Multi-Objective Optimization using Evolutionary Algorithms. John Wiley and Sons Publisher, London
[26] Aihara S 1987 A new running torque formula for tapered roller bearings under axial load. ASME J. Tribol. 109: 471–478
[27] IS 3824: 2002 Bureau of Indian Standard, Rolling bearings-Dynamic load ratings and rating lives
[28] Hamrock B J 1994 Fundamentals of Fluid Film Lubrication. McGraw-Hill, New York
[29] SKF, General Catalogue 2005 Media print, Germany